[American Journal of Science, Vol. 319, April, 2019, P. 287-314, DOI 10.2475/04.2019.02]

MAFIC WHOLE-ROCK GEOCHEMISTRY AND NEODYMIUM ISOTOPES, GREEN MOUNTAIN AND ROWE/PROSPECT ROCK SLICES, VERMONT APPALACHIANS

IAN W. HONSBERGER*,***,†, RAYMOND A. COISH**, JO LAIRD***, and SHUANGQUAN ZHANG§

ABSTRACT. Mafic rocks containing sodic-calcic amphibole in the Green Mountain slice (GMS) and Rowe/Prospect Rock slice (R/PRS), Vermont Appalachians were originally subalkaline basalts emplaced as melts during Neoproterozoic rifting of Rodinia that led to the formation of the Iapetus Ocean basin. Relatively high degrees of partial melting of asthenosphere that was highly depleted in incompatible elements produced R/PRS magma(s), which may have been contaminated locally by continental crust and/or fluids. Trace element chemistry suggests that mafic bodies from different locations in the R/PRS may be fractionated magmatic equivalents. Mafic rocks in the GMS formed from magmas produced by relatively low degrees of partial melting of mantle that was relatively enriched in incompatible elements compared to depleted mantle. These enriched melts may have been derived from a plume and/or enriched lithospheric components, potentially continental crust, embedded in depleted upper mantle. A depleted mantle signature preserved locally in the GMS probably reflects increasing asthenospheric input during crustal thinning, opposed to crustal or fluid contamination.

Whole-rock minor and trace element data from the GMS and R/PRS are distinct from analyses of glaucophane schist from the Tillotson Peak Complex in northern Vermont, which may be exhumed Iapetan ocean floor. Exhumed mafic rocks in the GMS and R/PRS were formed as lower plate melts prior to relatively high pressure subduction zone metamorphism, providing evidence for subduction of the Laurentian margin, not subduction erosion. Low pressure greenschist facies mafic rocks that occur structurally between the GMS and R/PRS were sourced from depleted or highly depleted mantle in a supra-subduction zone environment, potentially a forearc or backarc basin; an ophiolitic origin is equivocal. Geochemical and isotopic data and interpretations are compatible with rift-related tectonomagmatic models for the peri-Laurentian realm of the northern Appalachians.

Key words: Vermont, geochemistry, neodymium isotopes, mafic rocks, Green Mountains, Iapetus Ocean, Laurentia, Rodinia, rifting, subduction

INTRODUCTION

The northern Appalachian orogen (fig. 1A) is composed of crustal-scale peri-Laurentian and peri-Gondwanan terranes that were assembled and deformed during the Paleozoic (Rodgers, 1970; van Staal and others, 1998; Hibbard and others, 2007; van Staal and Barr, 2012; Tremblay and Pinet, 2016; Karabinos and others, 2017; Macdonald and others, 2017). From west to east, the orogen is subdivided into distinct tectonostratigraphic zones based on spatial variations in Neoproterozoic to Early Paleozoic stratigraphy and structures (Williams, 1979; Hibbard and other, 2006). The Humber Zone (fig. 1A) includes allochthonous magmatic and sedimentary rocks of the Laurentian margin, and has been subdivided further into lower metamorphic grade (External) and higher grade (Internal) domains in Newfoundland (Cawood

* Geological Survey of Canada, Ottawa, Ontario, Canada K1A 0E8
** Geology Department, Middlebury College, Middlebury, Vermont 05753
*** Department of Earth Sciences, University of New Hampshire, Durham, New Hampshire 03824
§ Isotope Geochemistry and Geochronology Research Centre, Carleton University, Ottawa, Ontario, Canada K1S 5B6
† Corresponding author: ian.honsberger@canada.ca

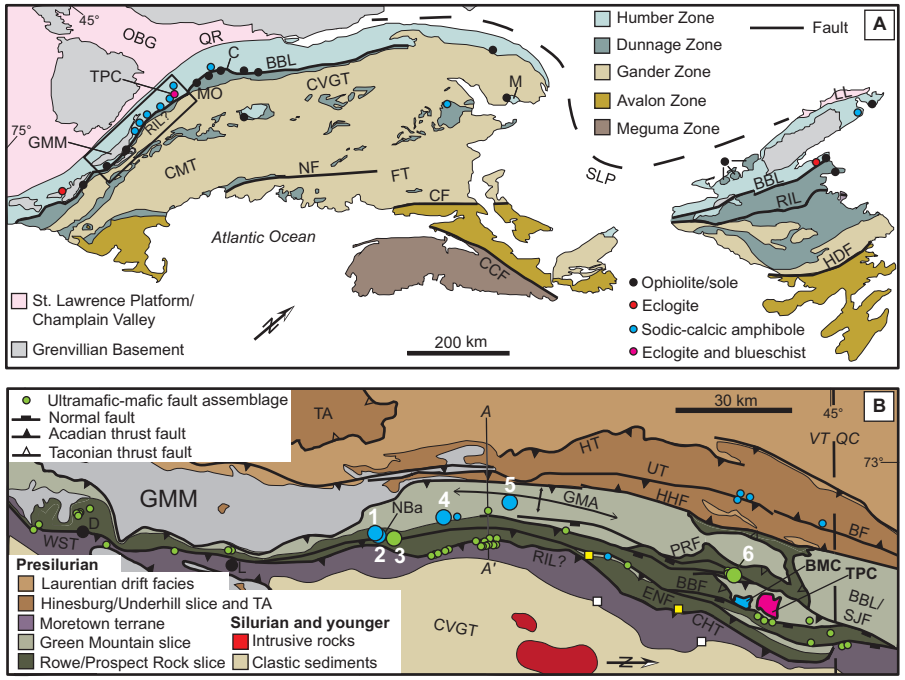

Fig. 1. (A) Generalized geologic map of the northern Appalachian orogen showing Presilurian lithostratigraphic zones and major faults (modified from Hibbard and others, 2006; Tremblay and Pinet, 2016). Note the zone in Vermont of mafic rocks containing sodic and sodic-calcic amphiboles of the Taconian subduction zone. The black rectangle encompasses the region shown in B. (B) Generalized geologic map of central and northern Vermont showing lithotectonic slices mentioned in text and major faults (modified from Ratcliffe and others, 2011; Karabinos and others, 2017). Blue circles and BMC mark locations of mafic rocks containing sodic-calcic amphiboles (barroisite/winchite). Locations of ultramafic-mafic±pelitic rock assemblages marked by green circles. Sample locations are shown as enlarged circles and numbered as follows: 1, Stockbridge; 2, Bethel; 3, Rochester; 4, Albee Brook; 5, Kew Hill; 6, Bowen Mountain. Reference data locations: white squares, Cram Hill and Moretown formations (Coish, 1997); yellow squares, Waterbury/Morrisville region (Coish and others, 2012). Ophiolitic ultramafic rocks in East Dover and Ludlow are marked by large black circles. Cross-section *A*-*A*′ shown in figure 2. Abbreviations: BBF, Burgess Branch fault zone; BBL, Baie Verte – Brompton Line; BF, Brome fault; BMC, Belvidere Mountain Complex; C, Caldwell Formation; CCF, Cobequid – Chedabucto fault; CF, Caledonia fault; CHT, Coburn Hill thrust; CMT, Central Maine terrane; CVGT, Connecticut Valley – Gaspe trough; D, East Dover; ENF, Eden Notch fault zone; FT, Fredericton trough; GMA, Green Mountain anticlinorium; GMM, Green Mountain Massif; HDF, Hermitage Bay – Dover fault; HHF, Honey Hollow fault; HT, Hinesburg thrust; L, Ludlow; LL, Logan's line; M, Maquereau Group; MO, Mount Orford; NBa, New Boston antiform; NF, Norumbega fault; OBG, Ottawa – Bonnechere Graben; PRF, Prospect Rock fault; QR, Quebec re-entrant; RIL, Red Indian Line; SJF, St. Joseph fault; SLP, St. Lawrence promontory; TA, Taconic allochthon; TPC, Tillotson Peak Complex; UT, Underhill thrust; WST, Whitcomb Summit thrust.

and others, 1994; Williams, 1995) and Quebec (Tremblay and Pinet, 1994). The Baie Verte – Brompton Line (Williams and St-Julien, 1982) marks the western boundary of the Dunnage Zone (fig. 1A), which consists of accreted peri-Laurentian and peri-Gondwanan arc terranes that are juxtaposed along a major tectonic suture in Newfoundland, the Red Indian Line (Williams and others, 1988). Farther east, the orogen is composed of accreted peri-Gondwanan microcontinents; Ganderia, Avalonia, and Meguma (fig. 1A).

Pre-Silurian metamorphosed mafic plutonic and volcanic rocks throughout the Humber and Dunnage Zones record magmatism during Neoproterozoic breakup of Rodinia and early Paleozoic closure of the Iapetus Ocean basin (Coish, 1997, 2010; van Staal and others, 1998). In the Dunnage Zone, such rocks are supra-subduction zone

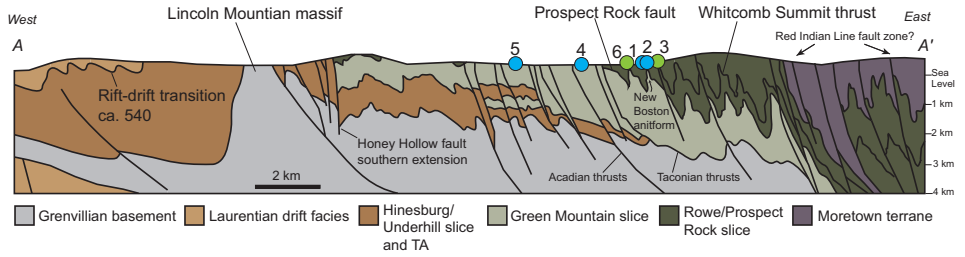

Fig. 2. Cross-section *A*-*A*′ (fig. 1B) with sample locations projected laterally onto the section. The polydeformed metamorphosed terrane from which samples were collected is characterized by shallowly- to moderately-dipping Taconian thrusts cut by steeply-dipping Acadian thrusts. Cross-section modified from Ratcliffe and others (2011).

arcs and rifted arcs of ophiolitic affinity (Zagorevski and others, 2007; van Staal and Barr, 2012; Tremblay and Pinet, 2016), whereas in the Internal Humber Zone mafic rocks were generated prior to Iapetan subduction during the latest stages of Rodinia rifting (Coish, 1997, 2010; Bédard and Wilson, 1997; Bédard and Stevenson, 1999; Cawood and others, 2001; Coish and others, 2012). Mafic magmatic rocks formed at the rift-drift transition (*ca.* 540 Ma; Cawood and others, 2001; Coish and others, 2012) are preserved west of peri-Gondwanan arc terrane (Moretown) in northern Vermont along the cryptic boundary between the Internal Humber Zone and Dunnage Zone.

The present research investigates the tectonomagmatic origin(s) of exhumed mafic rocks in central and northern Vermont (fig. 1B) that occur within the Green Mountain slice (GMS) and Rowe/Prospect Rock slice (R/PRS), which are correlative, respectively, with the Internal Humber Zone and the cryptic Internal Humber – Dunnage Zone boundary (Thompson and Thompson, 2003; Castonguay and others, 2012). These peri-Laurentian rocks preserve evidence for relatively high pressure subduction zone metamorphism associated with the closure of Iapetus (Laird and Albee, 1981a, 1981b; Laird and others, 1984, 1993; Honsberger and others, 2017). Whole-rock geochemistry and Nd isotopes indicate that the mafic rocks of this study are not ophiolitic but were derived from melts that were progressively depleted through time during continental extension of Rodinia. Crystallization of these rocks probably took place between *ca.* 571 Ma (Walsh and Aleinikoff, 1999) and *ca.* 540 Ma, the time of the Iapetan rift-drift transition (Cawood and others, 2001; Coish and others, 2012). Limited whole-rock data presented herein for low pressure greenschist at Bowen Mountain (Honsberger, ms, 2015) in northern Vermont are consistent with a supra-subduction zone affinity.

GEOLOGICAL AND STRUCTURAL CONTEXT

The northeast-trending structural grain of the northern Appalachians (fig. 1A) is inherited from the Neoproterozoic geometry of the Laurentian-Iapetan Ocean rift system (Rankin, 1976; Thomas, 2014). A thick pile (>2 km) of synrift sediments, slope-rise deposits, and rift-related magmatic rocks accumulated on the Laurentian margin in central and northern Vermont south of the Quebec re-entrant and Ottawa-Bonnechere graben (Thomas, 2014). This sedimentary-rich pile of rocks in Vermont comprising the Internal Humber Zone up to the Internal Humber Zone – Dunnage Zone boundary is now deformed, metamorphosed, and imbricated along thrust faults as allochthonous lithotectonic slices, from west to east: the Hinesburg/Underhill slice, GMS, and R/PRS (figs. 1B and 2; Stanley and Ratcliffe, 1985; Thompson and Thompson, 2003; Ratcliffe and others, 2011).

The Hinesburg thrust places the Hinesburg/Underhill slice (Internal Humber Zone) over peri-Laurentian drift facies rocks (figs. 1B and 2), which were in turn transported farther west in the hanging wall of the Champlain thrust (Ratcliffe and others, 2011). The Prospect Rock fault is a folded Taconian thrust that places the R/PRS on top of the GMS (figs. 1B and 2; Thompson and Thompson, 2003). The Honey Hollow thrust fault (fig. 1B) cuts the Prospect Rock fault along the Underhill slice – GMS contact (Ratcliffe and others, 2011). The Moretown terrane (Dunnage Zone), farther east and higher in the structural stack, truncates the R/PRS along a system of steep faults (figs. 1B and 2) that may be correlative with the Red Indian Line in Newfoundland (Macdonald and others, 2014, 2017; Karabinos and others, 2017). The Taconic allochthon occurs in southwestern Vermont (fig. 1B) above rocks of the Champlain Valley, but is rooted to the east near the R/PRS. Silurian-Devonian metasediments and intercalated metavolcanics and intrusions of the Connecticut Valley-Gaspé Trough in central and eastern Vermont unconformably and/or tectonically overlie the Moretown terrane (Westerman, 1987; Walsh and others, 2010).

Green Mountain and Rowe/Prospect Rock Slices

The GMS (Internal Humber Zone) consists of metamorphosed rift clastics, slope-rise sediments, and magmatic rocks that were deposited on the proto-Laurentian margin beginning in the Neoproterozoic and eventually subducted as part of the Iapetan slab in the late Cambrian to early Ordovician; these rocks comprise the Pinney Hollow, Fayston, and Hazens Notch formations in Vermont (Thompson and Thompson, 2003; Ratcliffe and others, 2011). The overlying Prospect Rock slice (Internal Humber – Dunnage zone boundary), as defined by Thompson and Thompson (2003) in central and northern Vermont, includes metamorphosed distal slope-rise deposits, oceanic sediments, and associated mafic and ultramafic bodies of the Jay, Ottauquechee, and Stowe Formations that overlie and are approximately the same age as rocks of the GMS. Correlative rocks south along strike in northwestern Massachusetts and southern Vermont are part of the Rowe belt, which occurs in the hanging wall of the Whitcomb Summit thrust and contains heterogeneous metamorphic assemblages and ultramafic lenses (Hatch and Stanley, 1976; Stanley and Hatch, 1988) similar to the Prospect Rock slice (Thompson and Thompson, 2003). In central and northern Vermont, Rowe schist is absent and the Stowe Formation occurs in the hanging wall of the Whitcomb Summit thrust (Ratcliffe and others, 2011). The Rowe belt and Prospect Rock slice are considered herein to be part of the same lithotectonic slice, the R/PRS, because they correlate structurally along strike and both contain imbricated rocks of an early Paleozoic accretionary prism that overrode the GMS (Stanley and others, 1984; Stanley and Ratcliffe, 1985; Stanley and Hatch, 1988).

Late Cambrian to Early Ordovician Tillotson Peak and Belvidere Mountain complexes (figs. 1A and 1B) in northern Vermont are eclogite to lower blueschist facies, respectively, ultramafic-mafic-pelitic subduction zone sequences that occur in the vicinity of the Prospect Rock fault structurally between the GMS and R/PRS (Laird and Albee, 1981a; Laird and others, 1984, 1993; Thompson and Thompson, 2003; Laird and Honsberger, 2013). The Prospect Rock fault is the closest analogue in Vermont to the Baie Verte-Brompton Line (fig. 1A) in southern Quebec; both are gently dipping deformed surfaces cut by steep normal faults (Thompson and Thompson, 2003; Tremblay and Pinet, 2016). The Burgess Branch fault zone (fig. 1B) cuts the Prospect Rock fault and is considered a southerly extension of the St. Joseph fault in southern Quebec (Kim and others, 2003; Tremblay and Pinet, 2016). The Eden Notch fault zone cuts the Prospect Rock fault farther east and structurally removes upper sections of the R/PRS east of the metadiabasic Mount Norris Intrusive Suite (Kim and others, 2003).

MAGMATIC CONTEXT

Whole-rock geochemistry of metamorphosed mafic rocks throughout peri-Laurentian terranes of the northern Appalachians reflects the Neoproterozoic to Early Paleozoic rift-related tectonomagmatic evolution of Rodinia and the Laurentian margin (Coish and others, 1991, 2012; Coish, 1997, 2010; Bédard and Wilson, 1997; Bédard and Stevenson, 1999; Cawood and others, 2001). In Vermont, magmatism during Rodinia breakup within the main pre-Iapetan rift basin is recorded by *ca.* 571 Ma felsic volcanics of the Pinney Hollow Formation (Walsh and Aleinikoff, 1999). Off-axis rifting along the Laurentian margin involved eruption of the Tibbit Hill volcanics *ca.* 554 Ma (Kumarapeli and others, 1989; Cawood and others, 2001; Thomas, 2014). Greenstones and amphibolites in the GMS and R/PRS may have formed quasi-continuously throughout the Neoproterozoic leading up to the Iapetan rift-drift transition *ca.* 540 Ma (Coish, 2010; Coish and others, 2012) as the result of a superplume that existed beneath present day northern Vermont and southern Quebec (Puffer, 2002; Coish and others, 2012).

Late Cambrian (*ca.* 505 – 490 Ma) arc-like magmas of the Dunnage Zone (for example, Jenner and others, 1991; David and Marquis, 1994) were likely generated during early stages of east-directed subduction of Iapetus (for example, Kim and Jacobi, 2002). Late Cambrian to Early Ordovician forearc boninites identified throughout the Dunnage Zone (for example, Coish and others, 1982; Dunning and Krogh, 1985; Dunning and Pedersen, 1988; Jenner and others, 1991; Kim and Jacobi, 1996, 2002; Bédard and others, 1998) are not observed in central and northern Vermont. Middle to Late Ordovician forearc tholeiitic basaltic magmatism in southern Quebec and northern Vermont preserved as the Bolton Igneous Group (Mélancon and others, 1997), Mount Norris Intrusive Suite (Kim and others, 2003), Coburn Hill volcanics (Gale, 1980), and in the Cram Hill Formation and Moretown terrane is attributed to slab break off during late stages of east-directed subduction (Coish and others, 2015; Karabinos and others, 2017). Subsequent west-directed subduction between ~470 and ~445 Ma generated magmas in the Bronson Hill arc (Macdonald and others, 2014, 2017), with *ca.* 450 Ma volcanism potenially the result of flat slab subduction of an aseismic ridge (Jacobi and Mitchell, 2018). Silurian crustal extension (Rankin and others, 2007) associated with slab detachment and lithospheric delamination (Rankin and others, 2007; Coish and others, 2015) and/or slab rollback (Dorais and others, 2017) produced widespread ~420 Ma mafic magmas that intruded rocks of the Bronson Hill arc, Connecticut Valley – Gaspe trough, and Shelburne Falls arc.

SAMPLE LOCATIONS AND MINERALOGY

Eleven greenstone samples and one amphibolite sample were collected from six general locations in the GMS and R/PRS (figs. 1B and 2, table 1). Mineral chemistry was presented by Laird and others (1984) for mafic rocks from locations 4 and 5. Sample numbers for Stockbridge are consistent with Honsberger and others (2017).

Four samples were collected from the GMS; two from a greenstone body encased in albite schist of the Fayston Formation at Kew Hill (location 5), and two from a body surrounded by non-albitic muscovite-rich schist of the Pinney Hollow Formation in Albee Brook (location 4). Neither body is in contact with ultramafic rocks. Sampling in the R/PRS was focused in central Vermont on the eastern limb of the New Boston antiform (figs. 1B and 2), a local structure within the Rochester Quadrangle that exposes albite schist similar to the GMS (Walsh and Falta, 2001). Three samples (2 greenstone and 1 amphibolite) from the Ottauquechee Formation come from separate bodies of an exhumed ultramafic-mafic-pelitic sequence in Stockbridge (location 1; Honsberger and others, 2017). Two additional Ottauquechee samples are from separate bodies in Bethel township (location 2), less than ~5 km to the northeast of Stockbridge, that are in contact with albite schist and/or muscovite schist but not

TABLE 1

Location names, numbers (figs. 1B and 2), and sample numbers for greenstones in the GMS and R/PRS

Location	Stockbridge			Bethel		Rochester		Albee Brook		Kew Hill		Bowen Mtn
Location Number	1			2		3		4		5		6
Lithotectonic Slice	R/PRS	R/PRS	R/PRS	R/PRS	R/PRS	R/PRS	R/PRS	GMS	GMS	GMS	GMS	R/PRS
Sample Number	2	3	6	94	95	98	99	107	108	109	113	116
Alteration Index[1]	42.83	35.92	48.22	24.74	41.23	34.03	23.53	31.67	38.60	36.55	32.63	32.63
Easting	679353	679341	679316	680248	680497	680061	680407	672569	672400	671069	670994	686445
Northing	4851019	4850825	485475	4852027	4852354	4859119	4857953	4870781	4870844	4892041	4891884	4954206
Sample Number[2]								V254		V321		

[1] Defined as 100 × (MgO + K_2O)/(MgO + K_2O + CaO + Na_2O) in weight %. [2] Sample numbers of mafic rocks from Laird and others (1984) for which mineral chemistry was presented; these samples do not correspond to the UTM coordinates (NAD 83).

ultramafics. Two samples from the Stowe Formation were collected from a greenstone unit in contact with an ultramafic body in Rochester (location 3).

One greenstone sample comes from outcrop mapped as the Ottauquechee Formation at Bowen Mountain (location 6), just southwest of the Belvidere Mountain Complex (Thompson and Thompson, 2003; Ratcliffe and others, 2011). Bowen Mountain greenstone is part of a mafic-ultramafic lens that occurs structurally between the GMS and R/PRS (Thompson and Thompson, 2003) in the same relative position as the Belvidere Mountain and Tillotson Peak complexes, but is low pressure greenschist based on amphibole compositions that range from calcic magnesio-hornblende to actinolite (Honsberger, ms, 2015).

It is unclear from field and textural relationships if samples originated as extrusive or intrusive igneous rocks, although amphibolite from Stockbridge (sample 6) is more likely intrusive. The mineralogy of the different mafic samples is described by modal variations within the six-phase assemblage, titanite-quartz-albite-chlorite-amphibole-epidote (±biotite±carbonate±magnetite±rutile) (fig. 3A); however, amphibole is

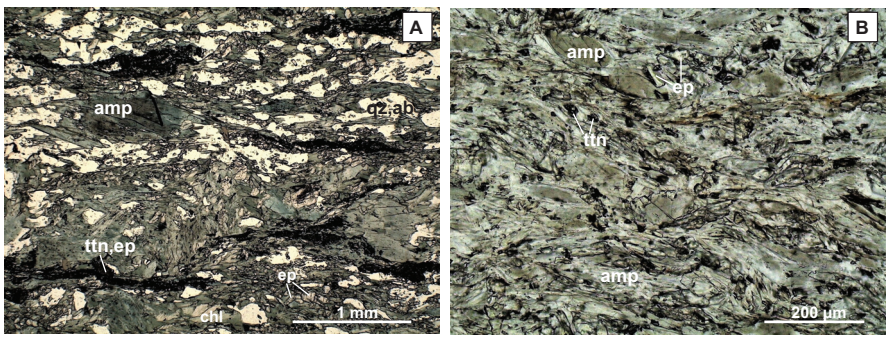

Fig. 3. Photomicrographs of mafic samples. (A) Photomicrograph of typical ttn-ab-qtz-chl-ep-amp greenstone from the GMS and R/PRS. The sample shown is from Albee Brook. The nearly horizontal deformation fabric is a transposed Taconian foliation. The labeled amphibole grain consists of a barroisite core and actinolite rim. (B) Photomicrograph of amphibole-rich, chlorite-poor Bowen Mountain greenstone. Amphibole occurs as both porphyroblasts and fine-grained matrix.

absent entirely from one Kew Hill (sample 113) and one Bethel sample (sample 95). In general, modal quartz and albite are greater where amphibole mode is less. Bowen Mountain greenstone is distinctive because it is exceptionally rich in amphibole and poor in chlorite compared to the other samples (fig. 3B). With the exception of Bowen Mountain, amphibole grains analyzed chemically are zoned outward from sodic-calcic (barroisite/winchite) cores to actinolite rims (fig. 3A), reflecting retrograde paths from upper greenschist – lower blueschist facies to lower greenschist facies (Laird and Albee, 1981b; Laird and others, 1984; Honsberger and others, 2017). Samples 3, 94, 95, 107, 108, 109, and 113 contain barroisite/winchite (Honsberger, ms, 2015; Honsberger and others, 2017). Bowen Mountain greenstone preserves amphiboles with low-Na magnesio-hornblende cores and actinolite rims, which are interpreted to reflect relatively low pressure facies series retrograde metamorphism (Honsberger, ms, 2015). Retrograde textures observed within the six-phase assemblage, titanite-quartz-albite-chlorite-amphibole-epidote, throughout north-central Vermont have been interpreted quantitatively to be the result of isochemical metamorphism involving the combination of closed-system net-transfer reactions and net-transfer reactions open to H_2O (Thompson and others, 1982; Laird and Thompson, 2005). Potential effects of major element mobility are discussed further in the section, MINOR AND TRACE ELEMENT GEOCHEMISTRY.

ANALTYICAL METHODS

Inductively Coupled Plasma Mass Spectrometry

Twelve fresh and homogenous double-fist-sized samples were cut with a water-cooled diamond blade, crushed dry in a ceramic jaw crusher, and powdered in a shatterbox with an aluminum sample chamber at Middlebury College, Vermont. To avoid contamination, the aluminum sample chamber was brushed, washed with deionized water and soap, cleaned with methanol, wiped dry with a kimwipe, and dried with compressed air between each sample. Powdered samples were prepared using lithium metaborate fusion techniques (Coish and Sinton, 1992). Samples were analyzed for SiO_2, TiO_2, Al_2O_3, Fe_2O_3(t), MnO, MgO, CaO, Na_2O, K_2O, P_2O_5 using a Thermo-ARL QUANT'X Energy Dispersive X-ray fluorescence spectrometer and for Sc, V, Cr, Co, Ni, Cu, Rb, Sr, Y, Zr, Nb, Ba, Zr, Y, Ba, As, La – Lu, Hf, Ta, Th, Th, Pb, and U (table 2) using a Thermo iCAPQ Inductively Coupled Argon Plasma Mass Spectrometer; both instruments are housed at Middlebury College.

Thermal Ionization Mass Spectrometry

Sm and Nd isotope ratios (table 3) were measured using a Thermo Finnigan's Triton thermal ionization mass spectrometer in Carleton University's Isotope Geochemistry and Geochronology Research Centre (IGGRC), Ottawa, Ontario. Silicate rock powders with a ^{148}Nd-^{149}Sm spike were dissolved in a mixed acid of ~29 M HF and ~16M HNO_3. Dissolved samples were dried down on a hotplate and subsequently re-dissolved sequentially in 8M HNO_3 and 6M HCl. Dried sample residues were dissolved in 2.5 M HCl and loaded into 14-ml Bio-Rad borosilicate glass chromatography columns containing 3.0 ml of Dowex AG50W-X8 cation resin. Columns were washed with 23 ml of 2.5 M HCl before REE were eluted using 9 ml of 6M HCl. REE fractions were dissolved in 0.26M HCl and loaded onto Eichrom Ln Resin chromatographic columns containing Teflon powder coated with HDEHP [di(2-ethylhexyl) orthophosphoric acid (Richard and others, 1976)]. Nd was eluted using 0.26M HCl, followed by Sm elution using 0.5M HCl.

Nd and Sm were loaded with H_3PO_4 in a double rhenium filament assembly for isotopic analyses at temperatures of 1500 to 1650 °C. Isotope ratios were normalized to $^{146}Nd/^{144}Nd = 0.72190$. An IGGRC in-house Nd standard measured routinely over a

TABLE 2

Whole-rock major, minor, and trace element chemistry for mafic samples from the GMS and R/PRS, Vermont and BCR-2

Locality		Stockbridge			Bethel		Rochester
Formation	Ottauquechee	Ottauquechee	Ottauquechee	Ottauquechee	Ottauquechee	Stowe	
Sample #	2	3	6	94	95	98	
SiO_2	41.87	47.37	43.26	46.27	44.91	49.22	
TiO_2	1.25	0.89	1.31	0.79	0.62	0.99	
Al_2O_3	14.38	14.93	13.80	15.54	13.59	14.32	
Fe_2O_3(t)	13.69	12.24	14.28	8.67	9.88	11.06	
MnO	0.25	0.19	0.28	0.16	0.18	0.16	
MgO	10.31	7.54	11.45	5.67	8.06	6.83	
CaO	13.42	11.66	11.10	15.62	9.85	10.52	
Na_2O	0.54	2.45	1.38	2.18	1.74	3.03	
K_2O	0.15	0.37	0.17	0.18	0.07	0.16	
P_2O_5	0.06	0.07	0.12	0.09	0.04	0.09	
LOI	3.01	2.64	3.50	4.91	10.42	3.54	
Total	98.93	100.34	100.65	100.08	99.36	99.92	
Sc	62.3	42.4	57.0	35.7	41.7	40.9	
V	370	321	437	248	272	289	
Cr	236	316	134	473	400	255	
Co	62.1	54.9	61.3	47.0	47.6	42.9	
Ni	120	132	101	185	114	103	
Cu	110	103	116	105	67.8	61.2	
Rb	2.8	12.9	2.8	4.5	0.4	4.2	
Sr	135	113	80.0	172	91.4	120	
Y	43.0	25.2	36.2	21.0	18.2	26.0	
Zr	50.5	50.7	74.6	52.3	31.7	56.4	
Nb	7.5	3.7	12.0	5.0	2.6	4.8	
La	6.7	4.0	6.0	3.5	1.8	3.9	
Ce	15.5	8.8	14.7	8.1	7.8	9.0	
Pr	2.3	1.3	2.1	1.2	0.7	1.3	
Nd	11.6	6.8	10.8	6.1	3.9	6.8	
Sm	4.5	2.2	3.6	2.1	1.5	2.4	
Eu	1.6	0.8	1.3	0.8	0.6	0.9	
Gd	6.5	3.3	4.9	3.0	2.3	3.4	
Tb	1.2	0.6	0.9	0.5	0.4	0.6	
Dy	8.1	4.4	6.2	3.6	3.2	4.4	
Ho	1.6	1.0	1.3	0.8	0.7	1.0	
Er	4.6	3.0	4.0	2.3	2.2	2.8	
Tm	0.6	0.4	0.6	0.3	0.3	0.4	
Yb	3.9	2.9	3.8	2.2	2.2	2.7	
Lu	0.5	0.4	0.6	0.3	0.3	0.4	
Hf	1.5	1.7	2.2	1.6	1.1	1.8	
Ta	0.6	0.2	0.8	0.3	0.1	0.3	
Th	1.9	0.7	0.7	0.4	0.2	0.6	

period of three years yield $^{143}Nd/^{144}Nd = 0.511831 \pm 0.000011$ (2σ), an equivalent value of $^{143}Nd/^{144}Nd = 0.511861 \pm 0.000009$ (2σ) for the La Jolla Nd standard. Uncertainties on Sm and Nd concentrations are estimated as less than 0.2 percent. Analyses of the USGS standard BCR-2 yield Nd = 28.53 ppm, Sm = 6.618 ppm, and

TABLE 2
(continued)

Locality	Rochester	Albee Brook		Kew Hill		Bowen Mt.
Formation	Ottauquechee	PH	PH	HN	HN	Ottauquechee
Sample #	99	107	108	109	113	116
SiO_2	45.13	49.17	48.46	46.00	44.76	48.79
TiO_2	0.85	1.77	0.63	2.17	3.15	1.31
Al_2O_3	13.13	14.09	14.82	15.54	14.66	14.43
Fe_2O_3(t)	9.52	11.97	10.07	15.28	16.34	10.87
MnO	0.15	0.18	0.16	0.20	0.22	0.18
MgO	5.67	6.16	8.23	6.00	4.02	7.13
CaO	16.10	9.42	10.68	8.58	8.48	12.36
Na_2O	2.65	4.13	2.60	2.46	2.75	2.65
K_2O	0.10	0.12	0.12	0.36	1.42	0.14
P_2O_5	0.08	0.14	0.05	0.18	0.11	0.10
LOI	5.97	2.70	3.79	3.11	2.76	2.01
Total	99.35	99.85	99.61	99.88	98.67	99.97
Sc	36.2	38.7	37.6	40.3	39.8	41.7
V	328.1	374.6	278.9	373.1	392.6	279.9
Cr	260.5	63.7	513.3	140.8	9.7	160.8
Co	41.0	47.2	47.1	49.6	48.1	31.2
Ni	98.1	60.2	132.6	74.4	30.1	27.0
Cu	54.7	110.6	65.3	97.2	87.9	60.6
Rb	1.6	0.7	1.1	6.9	18.2	1.4
Sr	164.9	204.8	84.2	346.5	358.6	178.4
Y	23.9	26.6	18.6	38.3	40.9	25.9
Zr	54.0	132.8	30.4	188.5	243.5	83.4
Nb	4.0	11.1	2.0	13.9	17.0	1.7
La	3.5	12.3	1.5	15.3	18.5	3.1
Ce	8.4	29.4	4.1	35.6	46.9	10.1
Pr	1.2	4.1	0.7	5.0	6.2	1.7
Nd	6.6	19.0	4.0	23.6	28.5	9.7
Sm	2.3	4.9	1.5	6.2	7.6	3.4
Eu	0.8	1.6	0.6	2.2	2.5	1.3
Gd	3.4	5.3	2.4	7.1	8.3	4.4
Tb	0.6	0.8	0.4	1.2	1.4	0.8
Dy	4.4	4.9	3.2	7.2	8.3	5.1
Ho	1.0	1.0	0.7	1.4	1.6	1.1
Er	2.9	2.7	2.2	4.0	4.5	3.1
Tm	0.4	0.4	0.3	0.6	0.6	0.4
Yb	2.8	2.4	2.2	3.6	4.1	2.9
Lu	0.4	0.4	0.3	0.5	0.6	0.4
Hf	1.7	3.9	1.0	5.4	7.3	2.5
Ta	0.2	0.8	0.0	1.0	1.4	0.0
Th	0.5	1.4	0.1	1.7	2.4	0.2

$^{143}Nd/^{144}Nd = 0.512643 \pm 0.000011$ (n = 13, 2σ). Total procedural blanks for Nd are less than 50 picograms. Initial εNd(t) values, which represent the amount of deviation from a chondritic uniform reservoir (Lugmair, 1974; DePaolo and Wasserburg, 1976) were calculated as by DePaolo (1981).

TABLE 2
(continued)

Sample #	Reference values BCR-2	Analyzed BCR-2	Percent Error
SiO_2	54.00	53.75	-0.5
TiO_2	2.27	2.32	2.2
Al_2O_3	13.48	13.57	0.7
Fe_2O_3(t)	13.77	14.03	1.9
MnO	0.20	0.19	-5.0
MgO	3.60	3.67	1.9
CaO	7.11	7.15	0.6
Na_2O	3.12	3.20	2.6
K_2O	1.77	1.79	1.1
P_2O_5	0.36	0.34	-5.6
Total	99.68	100	
Sc	33.5	33.8	0.9
V	417.6	432.7	3.6
Cr	15.9	15.2	-4.4
Co	37.3	38.4	2.9
Ni	12.6	16.4	30.2
Cu	19.7	19.3	-2.0
Rb	46.0	40.4	-12.2
Sr	337.4	350.1	3.8
Y	36.1	36.5	1.1
Zr	186.5	192.3	3.1
Nb	12.4	12.2	-1.6
La	25.1	26.2	4.4
Ce	53.1	54.7	3.0
Pr	6.8	7.0	2.9
Nd	28.3	29.8	5.3
Sm	6.5	6.9	6.2
Eu	2.0	2.0	0.0
Gd	6.8	7.2	5.9
Tb	1.1	1.1	0.0
Dy	6.4	6.6	3.1
Ho	1.3	1.3	0.0
Er	3.7	3.8	2.7
Tm	0.5	0.5	0.0
Yb	3.4	3.5	2.9
Lu	0.5	0.5	0.0
Hf	5.0	5.2	4.0
Ta	0.8	0.8	0.0
Th	5.8	6.3	8.6

Major oxides reported in wt%, trace elements in parts per million (ppm). Percent error = ((analyzed-reference)/reference)*100. PH = Pinney Hollow; HN = Hazens Notch.

MINOR AND TRACE ELEMENT GEOCHEMISTRY

Chemical Effects of Alteration

Research has shown that K_2O, Na_2O, MgO, CaO, SiO_2 and some trace elements such as Rb, Sr, and Ba are mobilized during metamorphism (for example, Humphris and Thompson, 1978; Mottl, 1983; Dostal and others, 1989; Wilson, 1989), whereas

TABLE 3

Neodymium isotopes for mafic samples from the GMS and R/PRS, Vermont

Locality	Sample	Fm.	Slice	Sm (ppm)	Nd (ppm)	$(^{147}Sm/^{144}Nd)_m$	$(^{143}Nd/^{144}Nd)_m$	$(^{143}Nd/^{144}Nd)_i$	$(^{143}Nd/^{144}Nd)_{CHUR}(t)$	$\varepsilon_{Nd}(t)$
1	2	Ot	R/PRS	5.051	13.45	0.2270	0.512968	0.512150	0.511929	4.3
	3	Ot	R/PRS	3.352	10.01	0.2025	0.512922	0.512192	0.511929	5.1
	6	Ot	R/PRS	3.652	12.15	0.1818	0.512950	0.512295	0.511929	7.1
2	94	Ot	R/PRS	2.321	7.029	0.1996	0.513023	0.512304	0.511929	7.3
	95	Ot	R/PRS	1.669	4.508	0.2239	0.513133	0.512326	0.511929	7.8
3	98	Stowe	R/PRS	3.726	11.01	0.2047	0.512977	0.512240	0.511929	6.1
	99	Stowe	R/PRS	2.401	6.911	0.2100	0.513019	0.512262	0.511929	6.5
4	107	PH	GMS	4.982	19.93	0.1511	0.512709	0.512164	0.511929	4.6
	108	PH	GMS	1.812	4.197	0.2284	0.513099	0.512276	0.511929	6.8
5	109	HN	GMS	7.263	27.37	0.1604	0.512689	0.512111	0.511929	3.6
	113	HN	GMS	6.893	26.23	0.1589	0.512711	0.512138	0.511929	4.1
6	116	Ot	R/PRS	3.566	10.58	0.2038	0.513026	0.512292	0.511929	7.1

$(^{143}Nd/^{144}Nd)_{CHUR}(t) = 0.512638 - 0.1967[(\exp \lambda_{Sm}(t)) - 1]$.

$\varepsilon_{Nd}(t) = 10^4[((^{143}Nd/^{144}Nd)_i / (^{143}Nd/^{144}Nd)_{CHUR}(t)) - 1]$. t = 550 Myrs; m = measurement; i = initial; HN = Hazens Notch; Ot. = Ottauquechee; PH = Pinney Hollow.

rare earth elements and high field strength elements including Zr, Y, Nb, Hf, Ta, Ti, and P are considered to be relatively immobile. Considering greenschist to upper greenschist facies metamorphism of the samples collected in this study, major and minor element mobility is evaluated. Major element mobility is assessed with an alteration index, $100 \times ((MgO + K_2O)/(MgO + K_2O + CaO + Na_2O))$ (wt %), with values between 28 and 44 representing relatively unaltered basalt, values less than 28 representing albitized basalts, and values greater than 44 representing chloritized basalts (Hashiguchi and others, 1983; Laflèche and others, 1993). Alteration indices for our samples range between 24 and 48 (table 1 and fig. 4). Sample 94 (Bethel) and sample 99 (Rochester) fall within the albitized basalt field and sample 6 falls within the chloritized field, whereas all other samples plot within the unaltered basalt field (fig. 4). For comparison, alteration indices calculated for six samples of glaucophane schist from the Tillotson Peak Complex (Laird and others, 2001) range between 28 and 39, thus, all samples fall within the unaltered basalt field (fig. 4). Alteration indices calculated for seven mafic samples from the Belvidere Mountain Complex (Doolan and others, 1982; Laird and others, 2001) range between 26 and 42 (fig. 4), with only one sample plotting in the albitized basalt field. The application of this alteration index to other metamorphosed mafic rocks in the northern Appalachians (for example, Laflèche and others, 1993; Kim and Jacobi, 1996; Coish and others, 2012) has further shown that the majority of mafic rocks throughout the host terranes of the present study are within the unaltered range for major elements. Because major oxides (MgO, CaO, N_2O, K_2O) may have been mobilized locally throughout the terrane (fig. 4, samples 6, 94, and 99); however, these elements are not utilized to interpret igneous processes in this research.

Minor and trace element mobility is assessed using plots of Zr, considered to be immobile during metamorphism (Floyd and Winchester, 1978; Pearce and Norry, 1979; Rollinson, 1993), against a given element. Linear trends between Zr and TiO_2, Y, Nb, and Yb for our samples (fig. 5) suggest that these elements were relatively immobile during metamorphism and, thus, are utilized herein to interpret igneous processes. Application of V and Sc to igneous discrimination is avoided herein based on irregular scatter on Zr plots (fig. 5).

Reference Data

Geochemical discrimination has been central to interpreting tectonomagmatic origins of metamorphosed mafic rocks throughout central and northern Vermont (for

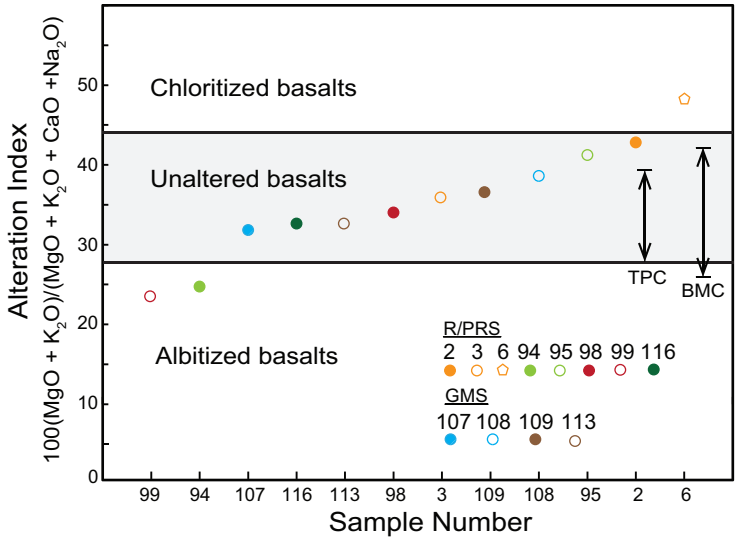

Fig. 4. Major element alteration indices (100 × ((MgO + K_2O)/(MgO + K_2O + CaO + Na_2O)) (wt %); Hashiguchi and others, 1983) for the twelve samples collected in this research. Black, double-headed arrows show range of alteration indices for Tillotson Peak Complex (TPC, left arrow) and Belvidere Mountain Complex (BMC, right arrow); data from Doolan and others (1982) and Laird and others (2001).

example, Coish and others, 1985, 1986, 1991, 2012, 2015; Coish, 1997, 2010; Kim and others, 2003; Rankin and others, 2007). New geochemical data herein (table 2) are interpreted with respect to published regional data. Two datasets that record rift-drift magmatism are from the Stowe and Hazens Notch formations in the Morrisville/Waterbury region (fig. 1B; Coish and others, 2012): 1) greenstones and amphibolites that formed as depleted to slightly LREE-enriched subalkaline to alkaline basalts (denoted Waterbury depleted); 2) greenstones that formed as highly LREE-enriched alkaline basalts (denoted Waterbury enriched). Datasets from greenstones in the Pinney Hollow, Hazens Notch, and Ottauquechee formations throughout central and northern Vermont are from Coish (1997, 2010), whereas data for the Cram Hill Formation (fig. 1B) in north-central Vermont are from Coish and others (2015). Data for Belvidere Mountain amphibolite come from Doolan and others (1982) and Laird and others (2001). N-MORB-like data from glaucophane schist of the Tillotson Peak Complex and data from one greenstone sample from Bowen Mountain come from Laird and others (2001).

Data for N-MORB along the southern portion of the Central Indian Ridge (Murton and others, 2005) and LREE-enriched basalt data from the Afar region, Ethiopia (Barrat and others, 2003) are also utilized. The southern segment of the Central Indian Ridge was chosen because its present position near the rift-rift-rift Rodrigues Triple Junction (Murton and others, 2005) is comparable to the Neoproterozoic position of Vermont metabasalts with respect to the Ottawa-Bonnechere graben-Iapetan rift system intersection (Burton and Southworth, 2010), interpreted as an ancient rift-rift-rift triple junction (Kumarapeli and others, 1989; Abdel-Rahman and Kumarapeli, 1999). Data from the Afar region are included because they have proved useful in interpretation of mafic magmatism at the Iapetan rift-drift transition (Coish and others, 2012). All sample and reference data are normalized to the same chondrite

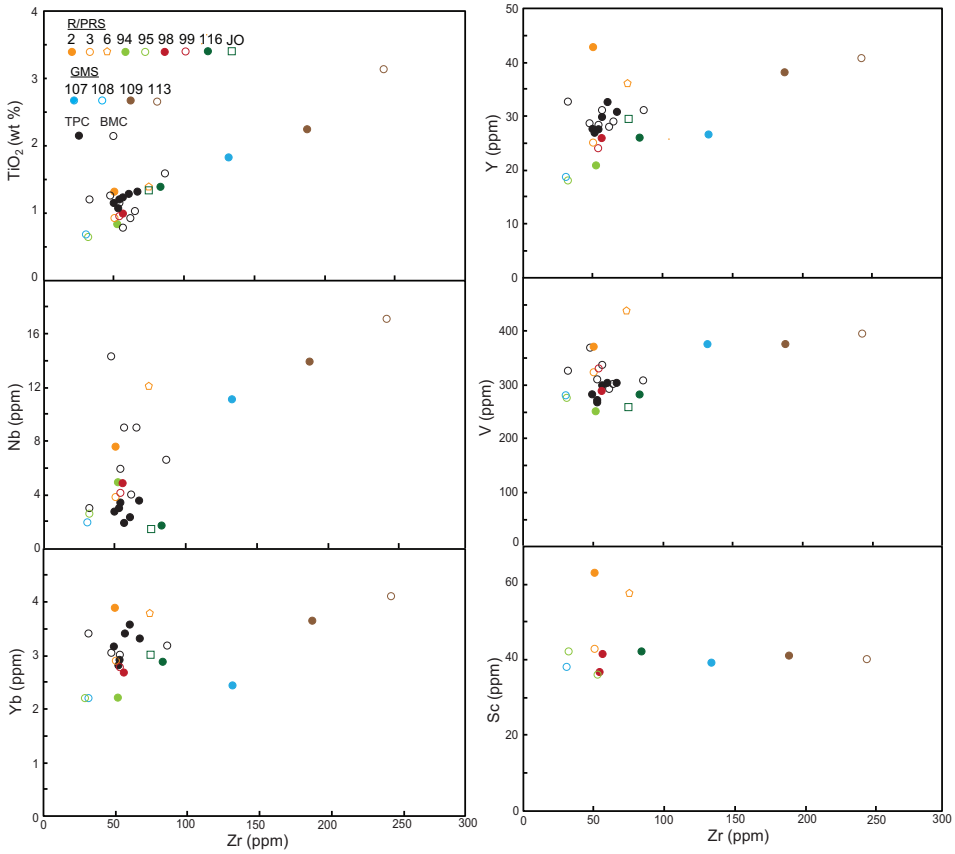

Fig. 5. Zr plots for all samples and selected reference data. Reference data include Belvidere Mountain Complex, Tillotson Peak Complex, and Bowen Mountain from Laird and others (2001); Sc was not reported in these datasets, thus, do not appear on the Sc vs Zr plot. Legend shows all the samples plotted. BMC, Belvidere Mountain Complex; JO, Bowen Mountain sample from Laird and others (2001); TPC, Tillotson Peak Complex.

(McDonough and Sun, 1995) and average N-MORB (Sun and McDonough, 1989) values.

Rare Earth and Extended Rare Earth Element Diagrams

Figure 6 (Nb/Y vs. Zr/TiO_2, Floyd and Winchester, 1978) shows that the samples are mainly subalkaline basalts to basaltic andesites, consistent with the majority of data published previously for metamorphosed mafic rocks in the GMS, R/PRS, and Belvidere Mountain and Tillotson Peak complexes. Figure 7A shows chondrite-normalized REE patterns for samples that are depleted ($(La/Yb)_n < 1$) to undepleted or slightly enriched ($(La/Yb)_n \sim 1 - 1.2$) in LREE. Datasets from the Belvidere Mountain Complex, Tillotson Peak Complex, and Waterbury/Morrisville region display similar patterns. The Tillotson Peak Complex and Central Indian Ridge N-MORB are both depleted in LREE compared to heavy rare earth elements (HREE), but Tillotson Peak Complex is slightly more enriched in La and Ce and between Gd and Lu. The HREE data range for Belvidere Mountain Complex is nearly identical to that for Tillotson Peak Complex but shows more variation in LREE towards enriched values (Laird and others, 2001).

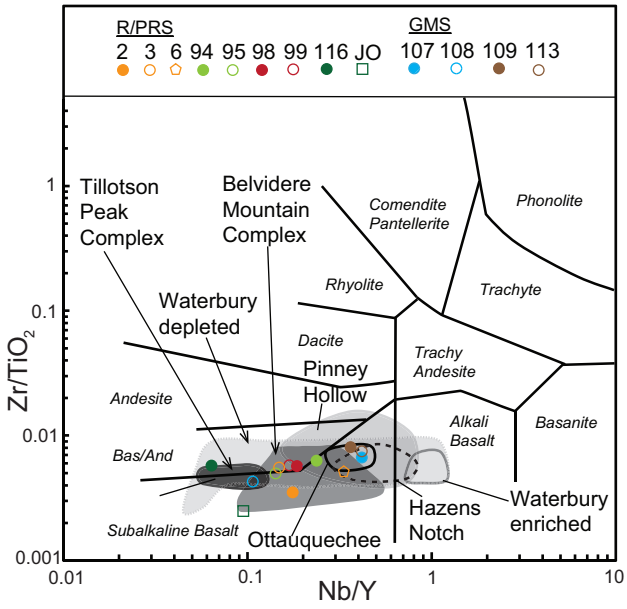

Fig. 6. Nb/Y vs Zr/TiO_2 diagram (Floyd and Winchester, 1978) showing that the majority of metamorphosed mafic rocks within the GMS and R/PRS are subalkaline basalts and basaltic andesites. Sample data are plotted as colored circles according to the legend in the upper left corner. Fields for reference data are also shown and labeled. JO = Bowen Mountain sample from Laird and others (2001).

REE concentrations for LREE-depleted to slightly enriched samples generally range between ~6× and 32× chondrite and ~0.6x and 7× N-MORB (figs. 7A and 7B), with samples 2 and 6 from Stockbridge being the most enriched in REE overall. These samples display U-shaped patterns between Th and Ti and nearly flat patterns between Gd and Yb. Both Rochester samples (98, 99) are nearly in unity with N-MORB between Pr and Yb but increasingly enriched from Ce to Th. Tillotson Peak data are similar

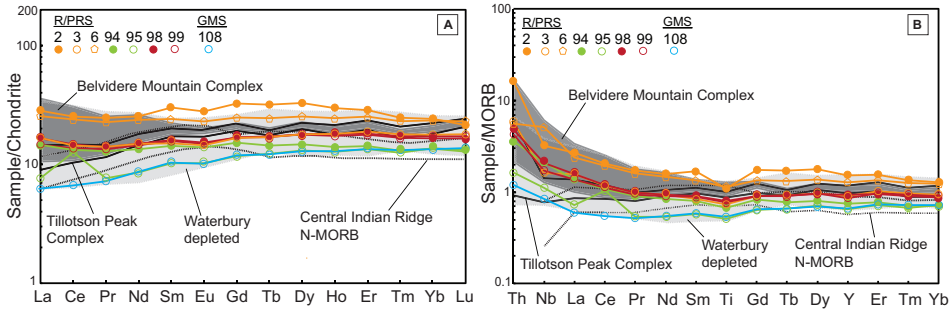

Fig. 7. (A) Chondrite-normalized (McDonough and Sun, 1995) REE plot for LREE-depleted to slightly enriched samples and reference data. Reference data plotted include the Tillotson Peak and Belvidere Mountain complexes (Laird and others, 2001), Waterbury/Morrisville LREE-depleted samples, and Central Indian Ridge N-MORB. Tillotson Peak data range falls between black solid lines, whereas Central Indian Ridge N-MORB data fall within dotted black lines. Pr, Gd, Dy, Er, and Tm were not reported for the Hazens Notch and Pinney Hollow samples. The legend includes all samples that are plotted. (B) MORB-normalized (Sun and McDonough, 1989) plot for the same samples and reference data shown in figure 7A.

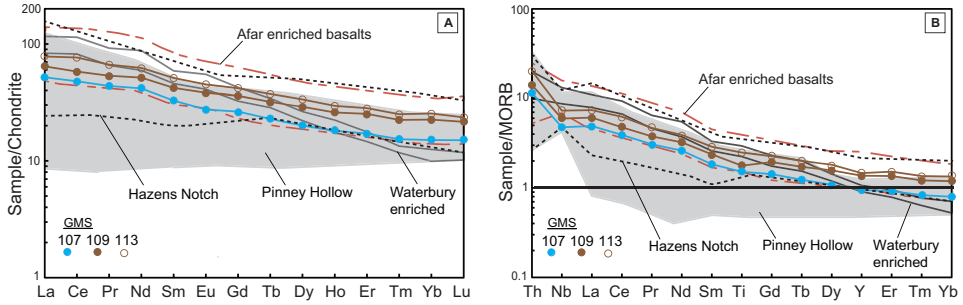

Fig. 8. (A) Chondrite-normalized (McDonough and Sun, 1995) REE plot for LREE-enriched samples (GMS) and reference data. Reference data shown are Hazens Notch, Pinney Hollow, and Afar enriched basalts. Afar enriched data falls between long-short dashed red lines. Pr, Tb, Ho, and Tm were not reported for the Afar basalts. Legend shows all samples that are plotted. (B) MORB-normalized (Sun and McDonough, 1989) plot for the same samples and reference data shown in figure 8A.

except for slight enrichment compared to N-MORB between Ti and Yb. Both Bethel samples (94, 95), sample 3 from Stockbridge, and Albee Brook sample 108 display patterns similar to Rochester samples (98, 99), but at slightly lower values. Samples 94, 95, and 108 are consistent with Central Indian Ridge N-MORB data between Tb and Yb.

Figures 8A and 8B show chondrite- and N-MORB-normalized diagrams, respectively, for samples relatively enriched in LREE compared to HREE ($(La/Yb)_n \sim 2-3$); these include samples 107 (Albee Brook), 109 (Kew Hill), and 113 (Kew Hill). Sample 107 (Albee Brook) displays a steeper REE pattern, but at lower values overall, than Kew Hill samples 109 and 113 (fig. 8A). Sample data are comparable to moderately to highly LREE-enriched greenstones in the Pinney Hollow, Hazens Notch, and Stowe Formations, including the Waterbury/Morrisville region, and all three samples fall within the Afar field (fig. 8A). Basalts from the Afar region are moderately enriched in LREE compared to the Waterbury/Morrisville dataset, and are comparable overall to the most LREE-enriched samples from the Pinney Hollow and Hazens Notch Formations.

Kew Hill samples (109, 113) are enriched with respect to N-MORB for the elemental spectrum (fig. 8B). Albee Brook sample 107 is enriched with respect to N-MORB between Th and Dy but slightly depleted between Y and Yb. Steep positive slopes are displayed between Th and Nb for all three samples; Nb anomalies are not observed (fig. 8B). A similar pattern, but steeper overall, is observed for the Waterbury/Morrisville data.

Bowen Mountain sample 116 and the sample analyzed by Laird and others (2001) preserve $(La/Yb)_n$ values less than 1 ($\sim$0.67–0.74) and display REE patterns that are slightly concave down between $\sim$10$\times$ and 11$\times$ chondrite (fig. 9A). N-MORB-normalized patterns for both samples are relatively flat and nearly in unity with N-MORB (fig. 9B), inconsistent with boninitic affinity. The lack of LREE depletion (fig. 9A) further distinguishes these samples from boninites of the Lac Brompton-Thetford Mines-Asbestos ophiolite belt in southern Quebec (Schroetter and others, 2005; De Souza and others, 2008; Tremblay and Pinet, 2016). Prominent negative Nb anomalies are preserved in both samples (fig. 9B), similar to metamorphosed mafic rocks in the Cram Hill Formation and Moretown terrane in northern Vermont that are interpreted to have formed via extension in a supra-subduction zone environment (Coish and others, 2015). The MORB-like signature of Bowen Mountain bears similarity to some tholeiitic sills of the Charlemont Intrusive Suite, which intrudes the eastern part of the Hawley Formation in northwestern Massachusetts and is interpreted to have been emplaced during Ordovician backarc extension (Kim and Jacobi, 1996).

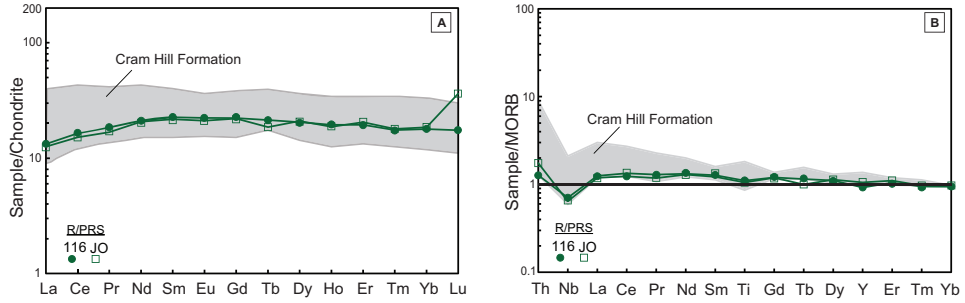

Fig. 9. (A) Chondrite-normalized (McDonough and Sun, 1995) REE plot for Bowen Mountain greenstone and Cram Hill Formation reference data (gray field). Legend shows all samples that are plotted. JO = Bowen Mountain sample from Laird and others (2001). (B) MORB-normalized (Sun and McDonough, 1989) plot for the same samples and reference data shown in figure 9A.

NEODYMIUM ISOTOPIC COMPOSITIONS

Reference Data

Neodymium isotope reference data come from two previous geochemical studies of pre-Silurian metamorphosed mafic rocks in Vermont. Coish (1997) presented data for the Pinnacle (2 samples), Underhill (3 samples), and Stowe (5 samples) formations, whereas Shaw and Wasserburg (1984) presented data for one sample of Belvidere Mountain amphibolite. An age of 550 Ma was used to calculate initial εNd(t) values for the Pinnacle and Underhill Formations, whereas 530 Ma was applied in calculations for the Stowe Formation (Coish, 1997). Shaw and Wasserburg (1984) used 500 Ma for Belvidere Mountain.

εNd(t) Values

Neodymium isotope concentrations were measured in all twelve samples (table 3, figs. 10A and 10B). Initial εNd(t) values were calculated with respect to 550 Ma, consistent with crystallization prior to the rift-drift transition *ca.* 540 Ma. These data are compared to some reference samples corrected to 530 Ma (Coish, 1997) and 500 Ma (Shaw and Wasserburg, 1984); the effect of 20 to 50 Myr age differences on initial εNd(t) values is ≤ 6 percent difference for all samples (less than the height of symbols in figs. 10A and 10B).

The εNd(550) values for our samples range from +3.55 to +7.75 (fig. 10A). Values for the three LREE-enriched samples (107, 109, 113; fig. 8A) and Stockbridge samples 2 and 3 are well below those for depleted mantle at 550 Ma, whereas both Rochester samples (98, 99) and Albee Brook sample 108 fall just below depleted mantle (fig. 10A). Samples 6 (Stockbridge), 94 (Bethel), and 116 (Bowen Mountain) plot just above the depleted mantle curve (fig. 10A). Sample 95 from Bethel falls farther above the depleted mantle curve, as does Belvidere Mountain amphibolite and most mafic rocks of the Stowe Formation (fig. 10A). Generally, the samples with the lowest εNd(550) values are most enriched with respect to LREE (figs. 8 and 10), demonstrating internal consistency between trace element and isotopic data.

The following ranges were reported by Coish (1997): Pinnacle (+3.1 to +3.2, εNd(550)); Underhill (+2.5 to +5.4, εNd(550)); Stowe (+6.9 to +9.2, εNd(530)). The εNd(500) value for Belvidere Mountain amphibolite is +8 (Shaw and Wasserburg, 1984).

Figure 10B is a compilation of εNd(t) values grouped with respect to pre-Silurian formation, and arranged west to east according to depositional proximity to Laurentia

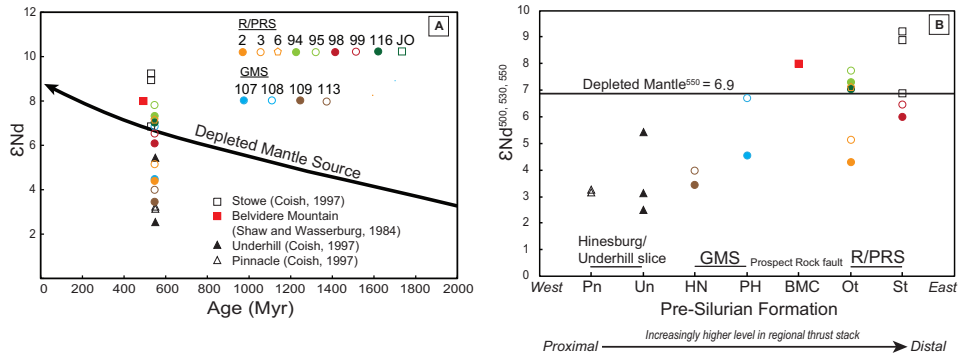

Fig. 10. εNd plots. (A) εNd values vs Age (Myr) for samples and reference data. The depleted mantle curve is from DePaolo (1981). Initial εNd values for all samples collected in this study were calculated with respect 550 Myrs. The following ages were utilized for reference data calculations: Belvidere Mountain (500 Myrs, Shaw and Wasserburg, 1984); Stowe Formation (530 Myrs, Coish, 1997); Underhill and Pinnacle Formations (550 Myrs, Coish, 1997). Legend shows all samples that are plotted. JO = Bowen Mountain sample from Laird and others (2001). (B) εNd values vs Pre-Silurian Formations. Formations are ordered from west to east by increasing level in the regional thrust stack, which corresponds to increasing distance of deposition with respect to the Laurentian margin. The depleted mantle εNd value corresponding to 550 Myrs (+6.9; DePaolo, 1981) is illustrated by horizontal black line; depleted mantle values corresponding to 500 (+7.1) and 530 (+7.0) Myrs are not illustrated. Reference data symbology the same as in figure 10A.

and depth within the regional thrust stack; higher level thrust slices that formed more distal to Laurentia plot toward the right. εNd(t) values generally increase towards more distal formations higher in the thrust stack, although, variation exists within individual formations (fig. 10B). εNd(550) data for the Pinnacle Formation are tightly clustered, whereas data for the Underhill Formation display a range of values (Coish, 1997). The Albee Brook greenstone body (Pinney Hollow Formation, samples 107 and 108) preserves dissimilar εNd(550) signatures between samples, whereas Kew Hill (Hazens Notch Formation, samples 109 and 113) does not show substantial within-body variation in εNd(550). Rochester samples (Stowe Formation, samples 98 and 99) have εNd(550) values that are less than those for other rocks analyzed in the Stowe Formation (Coish,1997). The six samples from the Ottauquechee Formation (samples 1, 2, 3, 94, 95, and 116) retain variable εNd(550) values. Thrust-bound bodies in Stockbridge (samples 2, 3, and 6) display ~3 units of variation in εNd(550) over only several hundred meters.

MANTLE ORIGINS

World-wide εNd(t) has increased systematically through time in the mantle source of continental crust due to protracted partial melting and accumulation of ^{147}Sm-^{143}Nd (DePaolo, 1981). εNd(t) values greater than the depleted mantle value at time (t) reflect generation from a highly depleted mantle source, whereas values lower than depleted mantle reflect formation from a more primitive mantle source and/or magma contamination by crust and/or fluids, which serves to decrease εNd(t) (DePaolo, 1981). Melting of primitive mantle produces depleted mantle (DePaolo, 1981), whereas melting of depleted mantle will give rise to highly depleted mantle (for example, Murphy and others, 2011, 2014).

Murphy and others (2014) interpreted highly depleted εNd(t) values for Iapetan supra-subduction zone mafic complexes to reflect melting of highly depleted oceanic plateau lithosphere that had experienced multiple phases of partial melting prior to incorporation above an Iapetan subduction zone. Bowen Mountain greenstones are the only potential supra-subduction zone rocks (fig. 9B) in the present study and they

plot along the depleted mantle curve (figs. 10A and 10B). This may suggest either a depleted mantle source, minor to moderate contamination of a highly depleted magma, or depleted partial melt contributions to highly depleted magma. Contamination of highly depleted magma to produce depleted magma may be the simplest explanation in light of regional isotopic interpretations (Murphy and others, 2014).

Highly depleted εNd(t) values recorded in the R/PRS (fig. 10B) imply formation from mantle that had experienced multiple previous episodes of partial melting, potentially during earlier stages of rifting. Mantle asthenosphere is a potential source for melts in the R/PRS because episodes of decompression melting that likely accompanied lithospheric thinning leading to Iapetan seafloor spreading can explain both depleted LREE signatures and highly depleted εNd(t) values (for example, Coish, 1997, 2010). Relatively low εNd(t) values preserved locally in the R/PRS in Stockbridge (samples 2 and 3) and Rochester (samples 98 and 99) may reflect crustal and/or fluid contamination of the magma because these samples deviate from the regional trend (10B) and are depleted or undepleted with respect to incompatible elements (figs. 7A and 7B), which is inconsistent with a primitive, more enriched mantle source. Outcrop-scale intercalation of mafic volcanic and plutonic rocks with mafic, pelitic, and psammitic sediments in these sample locations further supports crustal contamination of the magma. Chemical mobility due to metamorphism is ruled out based on linear trends on Zr plots (fig. 5).

Relative enrichment in incompatible elements (for example, fig. 8) coupled with relatively low εNd(t) values for metamorphosed mafic rocks in the Pinnacle, Underhill, and Hazens Notch (samples 109 and 113) formations (fig. 10B) may reflect either a plume influence, melting of enriched lithosphere, or crustal contamination of a more depleted melt. The systemic increase of εNd(t) values west to east across the lithotectonic slices (fig. 10B) is compatible with a progressive rift model that involves depletion of the melt source through time as the lithosphere thins (for example, Coish and others, 1991; Coish, 1997, 2010); therefore, relative enrichment of the Pinnacle, Underhill, and Hazens Notch (samples 109 and 113) formations is more likely a function of the melt source (plume or enriched lithosphere), opposed to crustal contamination. Even though the regional geochemical trend is probably related to the melt source, it cannot be ruled out that crustal and/or fluid contamination caused variations in Nd isotopes within formations and/or individual bodies, such as samples 107 and 108 from the Pinney Hollow Formation (fig. 10B). Another possibility, perhaps more likely considering the regional rift evolution (for example, Coish, 1997, 2010), is that the mantle source was heterogeneous at the scale of a Formation or individual body. A modern example of heterogeneous mantle is that beneath Iceland, where a mantle plume and mid-ocean ridge are interacting (Fitton and others, 1997; Fitton, 2007), thus, provides a chemical framework for interpreting the nature of potentially heterogeneous mantle sources.

The Zr/Y vs Nb/Y diagram is effective for discriminating Icelandic E-MORB and enriched OIB mantle sources from incompatible element-depleted N-MORB mantle sources (fig. 11; Fitton and others, 1997; Fitton, 2007). N-MORB mantle sources are distinctly more depleted in Nb with respect to Zr and Y compared to Icelandic E-MORB and OIB, and thus plot below the Iceland array (Fitton and others, 1997). Average continental crust also plots below the array (fig. 11) but reflects more incompatible element-enriched partial melts compared to N-MORB. The degree of partial melting decreases with incompatible element enrichment from left to right across the diagram, with the lowest degree, most enriched partial melts on the far right and the highest degree, most depleted partial melts on the lower left (Fitton and others, 1997). Enriched OIB compositions reflect either a plume influence or melting of enriched portions of upper mantle (Fitton, 2007).

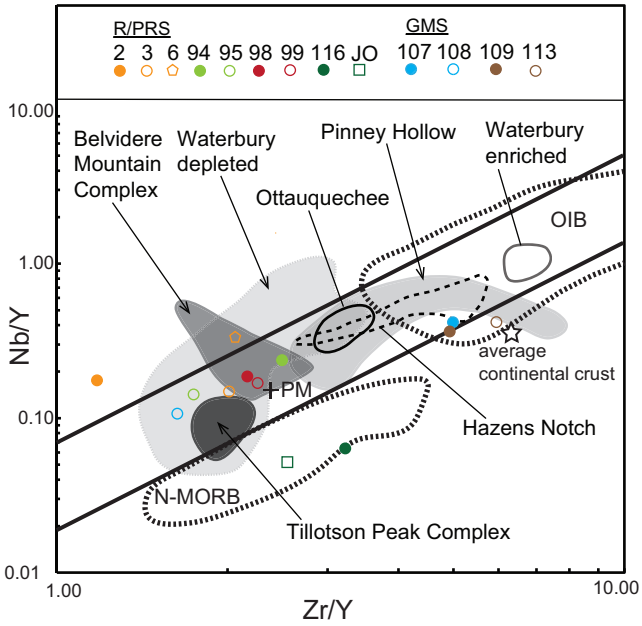

Fig. 11. Zr/Y vs Nb/Y diagram (Fitton and others, 1997; Fitton, 2007) that shows the range of data for the basaltic Iceland array (between straight black lines), N-MORB, and OIB. N-MORB and OIB data fall within the fields outlined by bold dotted lines in the lower left and upper right, respectively. Legend shows all samples that are plotted. JO, Bowen Mountain sample from Laird and others (2001); N-MORB, normal mid-ocean ridge basalt; OIB, ocean island basalt; PM, primitive mantle (McDonough and Sun, 1995); white star, average continental crust (Rudnick and Fountain, 1995; Barth and others, 2000).

Bowen Mountain samples reflect relatively high degrees of partial melting of an N-MORB mantle source (fig. 11). LREE-depleted patterns, negative Nb anomalies, relatively low Y, V, and Sc, and HREE concentrations for Bowen Mountain greenstone (figs. 9A and 9B) are consistent with supra-subduction zone melting of spinel peridotite that did not contain garnet (Pearce, 2008). Garnet is also interpreted to have been absent in the peridotite source(s) for LREE-depleted to slightly LREE-enriched samples from Stockbridge (1, 2 and 3), Bethel (94 and 95), Rochester (98 and 99) and Albee Brook (107 and 108). Depleted incompatible element concentrations in these rocks are consistent with relatively high degrees of partial melting of an E-MORB mantle source, similar to Belvidere Mountain amphibolite. Sample 2 from Stockbridge is strongly depleted in Zr relative to Y and plots well above the array, reflecting a mantle source more enriched in Nb compared to Icelandic E-MORB. Tillotson Peak data overlap the N-MORB boundary (fig. 11) and reflect a mantle source more similar to N-MORB than the E-MORB-like sample suite.

Kew Hill samples (109 and 113) and the LREE-enriched Albee Brook sample (107) plot in the OIB field on figure 11. LREE, TiO_2, Zr, and Nb enrichment in these samples (figs. 8A and 8B) are consistent with relatively low degrees of partial melting of an OIB-like source. HREE concentrations similar to MORB (fig. 8B) for these samples are inconsistent with the presence of garnet in the melt residue (Pearce, 2008). The relative depletion in Nb in these enriched samples compared to the Iceland array is consistent with a melt contribution from average continental crust (fig. 11).

Geochemical heterogeneity in Icelandic basalts is explained by mantle plume-ridge interaction (Fitton and others, 1997; Fitton, 2007). In Vermont, a *ca.* 571 Ma age

for volcanism in the Pinney Hollow Formation (Walsh and Aleinikoff, 1999) suggests that exhumed samples of this study were formed prior to development of the Iapetan mid-ocean ridge; thus, arguing against interaction of a plume with a fully developed mid-ocean ridge. The geochemical variations documented in metamorphosed basalts of the present research (for example, figs. 7–12) are consistent with a petrogenetic model involving interaction of a mantle plume with asthenospheric melts during progressive lithospheric extension of Rodinia, which eventually led to seafloor spreading and ridge development (for example, Coish, 1997, 2010). An alternative hypothesis not involving a plume is that the more incompatible element enriched components were sourced from low degree partial melts of enriched blobs, potentially continental crust, embedded in the depleted upper mantle (for example, Fitton, 2007). In either case, the eastward increase in $\varepsilon Nd(t)$ values across north-central Vermont (fig. 10B) is compatible with the temporal evolution of a mantle melt source from more enriched mantle for rocks in the GMS to highly depleted mantle for rocks in the R/PRS.

TECTONOMAGMATIC EVOLUTION

Potential effects of fractional crystallization of parental magmas are examined in plots of TiO_2, Y, Nb, and Yb vs Zr (fig. 5). Samples from the R/PRS (2, 3, 6, 94, 95, 98, 99) display relatively linear trends on these Zr plots, suggesting fractional crystallization from a common parent magma. Distinct linear trends for Tillotson Peak Complex reference data suggest fractional crystallization from a separate magma. Belvidere Mountain Complex reference data are scattered on Zr plots, which is interpreted to represent true chemical heterogeneity in the parent magma(s) because the major element alteration index (Hashiguchi and others, 1983; Laflèche and others, 1993) demonstrates that all but one Belvidere Mountain reference sample is consistent with unaltered basalt (fig. 4). Bowen Mountain sample 116 and the Bowen Mountain sample from Laird and others (2001) overlap similar values on Zr plots and do not show consistent linear trends with other samples (fig. 5). It is unclear if these samples are related by fractionation. Greenstones from Kew Hill and the Pinney Hollow Formation at Albee Brook define rough linear trends on Zr plots (fig. 5), suggesting that these rocks may be fractionated magmatic equivalents distinct from the R/PRS rocks. The absence of prominent negative Eu anomalies in all sample and reference data (figs. 7–9) suggests that early plagioclase fractionation did not occur within any of the magma systems.

Figure 12 (La/10 vs Y/15 vs Nb/8; Cabanis and Lecolle, 1989) demonstrates that mafic samples from the GMS and R/PRS were emplaced as magmas in extensional environments. Samples from the R/PRS (2, 3, 6, 94, 95, 98, 99) plot within the E-MORB field or along the boundary between N-MORB and E-MORB, similar to reference data from depleted Waterbury/Morrisville samples, Ottauquechee Formation, Belvidere Mountain, and most of the Pinney Hollow Formation (fig. 12). An evolved continental rift is the most likely extensional tectonic environment to explain generation of locally contaminated E-MORB melts derived from heterogeneous mantle during continental margin sedimentation (for example, Barrat and others, 2003). This is consistent with tectonomagmatic interpretations of greenstones and amphibolite elsewhere in the R/PRS (Coish, 1997, 2010), including in the Waterbury/Morrisville area where mafic magmatism at the rift-drift transition may be recorded (Coish and others, 2012).

Kew Hill samples (109 and 113) and one Albee Brook sample (107) plot within the continental basalts field close to the extensional E-MORB field and overlap compositions of Hazens Notch samples (fig. 12). Continental detritus and rift-related volcanics (Walsh and Aleinikoff, 1999) throughout the GMS (Ratcliffe and others, 2011) and incompatible element enrichment (figs. 8A, 8B, and 11) are consistent with

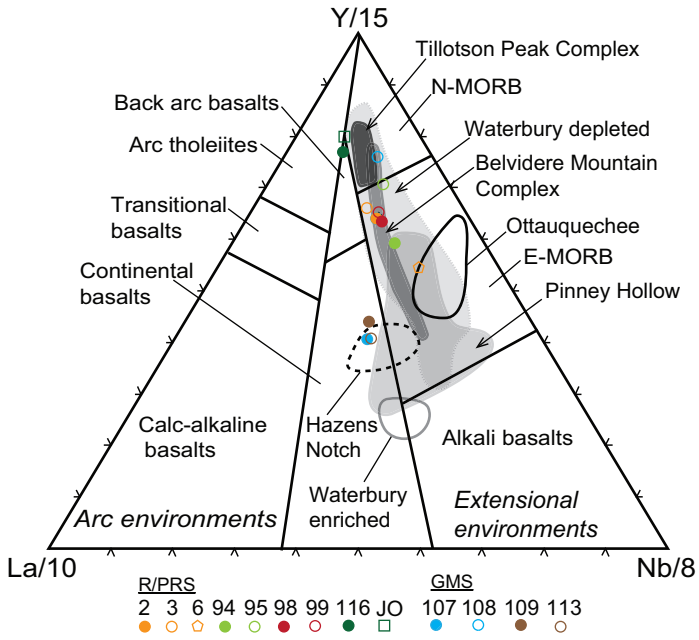

Fig. 12. La/10 vs Y/15 vs Nb/8 ternary discrimination diagram (Cabanis and Lecolle, 1989) that shows sample and reference data. Reference data plotted and labeled are Belvidere Mountain (Laird and others, 2001), Hazens Notch, Ottauquechee, Pinney Hollow, Tillotson Peak Complex, Waterbury/Morrisville LREE-depleted samples, and Waterbury/Morrisville LREE-enriched. Legend shows all data that are plotted. JO = Bowen Mountain sample from Laird and others (2001).

a continental rift setting for these greenstone samples. One Albee Brook sample (108) plots in the N-MORB field and one (107) plots in the continental basalts field (fig. 12), reflecting either interaction of different magmatic components in the formation of the mafic body, and/or crustal/fluid contamination of the magma. Magmatic interaction may also explain mafic magmas within the Underhill slice, which retain a relatively wide range of εNd(550) values (figs. 10A and 10B; Coish, 1997).

If mafic rocks in the GMS were generated prior to mafic rocks in the R/PRS (Coish, 1997, 2010), the data presented herein may capture the geochemical and isotopic evolution during Neoproterozoic continental rifting leading to the formation of the Iapetus Ocean, prior to the rift-drift transition (for example, Coish, 1997, 2010). In this context, relatively enriched mantle melts (GMS) beneath thinned continental lithosphere interact with depleted asthenospheric melts (R/PRS) as decompression melting becomes more prevalent during progressive rifting. Such a scenario is compatible with magmatism along the main pre-Iapetan rift *ca.* 571 Ma (Walsh and Aleinikoff, 1999; Coish, 2010). Metamorphosed basaltic lavas in the Caldwell Formation (Bédard and Stevenson, 1999) and Maquereau Group (Bédard and Wilson, 1997) along the Laurentian margin in Quebec and New Brunswick (fig. 1A), respectively, are correlative rocks that were also generated during the final stages of rifting of Rodinia. Maquereau Group lavas show evidence for crustal contamination (Bédard and Wilson, 1997), whereas isotopic data do not support crustal contamination of Caldwell Group lavas (Bédard and Stevenson, 1999).

Bowen Mountain samples plot along the boundary between backarc basin basalts and arc tholeiites (fig. 12); therefore, these samples are interpreted to have formed in an extensional arc setting. MORB-like REE patterns coupled with negative Nb anomalies

(fig. 9B) for Bowen Mountain samples are consistent with formation in a supra-subduction zone forearc or backarc basin. The protolith of Bowen Mountain greenstone, therefore, probably did not form until the early Ordovician during subduction of the Iapetus Ocean basin. Geochemical data from Bowen Mountain are similar to rocks of the Cram Hill Formation and Moretown terrane that are thought to have formed as a result of forearc magmatism during Early Paleozoic lithospheric delamination (Coish and others, 2015). It cannot be discounted that the Bowen Mountain greenstone body is an ophiolite fragment, but more geochemical data are required to test fully this hypothesis.

Tillotson Peak and Belvidere Mountain Complexes

Consistent incompatible element depletion, N-MORB-like geochemistry, and lack of supra-subduction zone signatures for glaucophane schist samples of the Tillotson Peak Complex (Laird and others, 2001) might indicate that the eclogite and blueschist facies rocks are exhumed remnants of subducted Iapetan ocean crust. If so, this would be the only such occurrence identified in the northern Appalachians. The lack of major element alteration and tight range of alteration indices for Tillotson Peak rocks (fig. 4) may suggest relatively fast exhumation following high pressure metamorphism. More geochemical data from the Tillotson Peak Complex are required to test these hypotheses. Eclogite of the Fleur de Lys Supergroup just west of the Baie Verte – Brompton Line in Newfoundland (fig. 1A) is a Neoproterozoic intrusive suite within Laurentian basement (Hibbard, 1983; Castonguay and others, 2014), whereas blueschist of the Bathurst Supergroup in New Brunswick is interpreted as an accreted seamount that was consumed during Silurian subduction (van Staal and others, 2008).

Based primarily on structural relationships, the Belvidere Mountain Complex has been correlated previously with ophiolitic soles in southern Quebec (Doolan and others, 1982; Kim and others, 2003; Tremblay and Pinet, 2016); a geochemical correlation is more ambiguous. Shaw and Wasserburg (1984) interpreted the $\varepsilon Nd(500)$ value of +8 for Belvidere Mountain amphibolite to reflect formation from oceanic crust. Minor element and REE data from Laird and others (2001) are not compatible with a supra-subduction zone affinity (no obvious arc signatures nor negative Nb anomalies). Lithological and structural similarities between the ultramafic-mafic-pelitic Tillotson Peak (Bothner and Laird, 1999) and Belvidere Mountain complexes (Gale, 1986, 2007) suggest a tectonic link between the two; although, Tillotson Peak Complex is more restricted geochemically (figs. 6–12). Belvidere Mountain amphibolite is more similar geochemically to mafic rocks in the R/PRS than it is to glaucophane schist at Tillotson Peak (figs. 6–12). Ultramafic rocks in these complexes and throughout the GMS and R/PRS undoubtedly retain key geochemical information regarding tectonomagmatic origins. Two serpentinized ultramafic bodies east of the Green Mountain Massif in East Dover and Ludlow (fig. 1B) retain supra-subduction ophiolitic mineral chemistries (Coish and Gardner, 2004).

CORRELATIONS BETWEEN MAGMATISM AND METAMORPHISM

The present research establishes a first-order correlation between tectonomagmatic setting and conditions of peak Taconian metamorphism for mafic rocks within and between the GMS and R/PRS. Mafic bodies containing barroisite/winchite in the GMS and R/PRS (Stockbridge, Bethel, Albee Brook, Kew Hill) crystallized originally as igneous rocks during intermediate to late stage continental rifting of Rodinia, before being subducted in the Early Paleozoic to at least ~35 to 40 Km depth (Honsberger and others, 2017). Mafic rocks that occur between the GMS and R/PRS along the Prospect Rock thrust (Tillotson Peak Complex, Belvidere Mountain Complex, and Bowen Mountain) are variable with respect to whole-rock geochemistry and metamorphic grade. Bowen Mountain greenstone is low pressure greenschist facies (Honsberger,

ms, 2015), the Belvidere Mountain Complex is probably upper greenschist to lower blueschist facies (medium-high pressure, Laird and others, 1993), and the Tillotson Peak Complex is blueschist to eclogite facies (Laird and Albee, 1981a). Low pressure at Bowen Mountain may be explained by early Ordovician obduction onto the Laurentian margin from a supra-subduction zone position, as is interpreted for ophiolites in southern Quebec (Tremblay and Pinet, 2016). Alternatively, Bowen Mountain may be an early Ordovician forearc intrusion related to slab break off, as is interpreted for rocks of the Bolton Igneous Group in southern Quebec (Mélancon and others, 1997) and Mount Norris Intrusive Suite in northern Vermont (Kim and others, 2003).

Melts emplaced during rifting of Rodinia (GMS, R/PRS, and Belvidere Mountain Complex) or within the Iapetus Ocean basin (Tillotson Peak Complex?) were on the lower plate during Taconian subduction and experienced higher pressure metamorphism than supra-subduction zone rocks of the upper plate (Bowen Mountain), with eclogite facies metamorphism of Iapetan ocean crust (Tillotson Peak Complex?). This implies that subduction of the Laurentian margin, not subduction erosion, was responsible for high pressure subduction zone metamorphism of exhumed mafic rocks throughout the GMS and R/PRS in Vermont.

Whole-rock geochemistry demonstrates that mafic rocks in Vermont containing barroisite are not retrograded magmatic equivalents of glaucophane schist of the Tillotson Peak Complex. Pressure-temperature paths of mafic rocks throughout the GMS and R/PRS, therefore, reflect subduction and exhumation histories of multiple lithospheric components. Local geochemical and metamorphic variations suggest that mafic-ultramafic-pelitic sequences (for example, Tillotson Peak Complex, Belvidere Mountain Complex, Stockbridge) within and between the GMS and R/PRS may be tectonic mélanges that were exhumed in a sediment- and/or serpentinite-rich channel (for example, Angiboust and others, 2013; Guillot and others, 2015). In such a model, the Belvidere Mountain and Tillotson Peak complexes may have been exhumed at different rates from different depths, but emplaced essentially side-by-side above the GMS and below the R/PRS.

CONCLUDING STATEMENT

Immobile trace element concentrations in the mafic rocks of study are consistent with crystallization of subalkaline basaltic melts produced during Neoproterozoic continental rifting of Rodinia. The $\varepsilon Nd(t)$ data presented document the interaction of depleted asthenosphere with enriched melts and, as well, progressive asthenospheric contributions during lithospheric extension that lead to the generation of Iapetan Ocean crust. Trace element and isotopic data herein are consistent with Neoproterozoic tectonomagmatic rift models for the Humber Zone and peri-Laurentian Dunnage Zone of the northern Appalachians (for example, Bédard and Stevenson, 1999; Coish, 2010); however, additional studies of exhumed mafic and ultramafic rocks throughout the orogen are required to understand more completely the mechanisms of generation, exhumation, and preservation.

ACKNOWLEDGMENTS

This research was conceived and samples were collected as part of IWH's Ph. D. thesis at the University of New Hampshire (Honsberger, ms, 2015). Whole-rock geochemical data were obtained during 2016 when IWH was working at Carleton University. Insightful geochemical discussions with Julie Bryce, Florencia (Prado) Fahnestock, and Hamish Sandeman are much appreciated. We gratefully acknowledge financial support from the Vermont Geological Society, Burlington Gem and Mineral Club, Jonathon Herndon, and University of New Hampshire Department of Earth Sciences for sample collection. A start-up grant to IWH from Carleton University funded major and trace element and isotope analyses. Critical reviews by Jonathan

Kim, Robert Jacobi, Benoit Saumur, an anonymous reviewer, and Associate Editor Robert Wintsch improved the manuscript. This is NRCan Contribution number 20180200.

REFERENCES

Abdel-Rahman, A. F. M., and Kumarapeli, P. S., 1999, Geochemistry and petrogenesis of the Tibbit Hill metavolcanic suite of the Appalachian fold belt, Quebec-Vermont: A plume-related and fractionated assemblage: American Journal of Science, v. 299, n. 3, p. 210–237, https://doi.org/10.2475/ajs.299.3.210

Angiboust, S., Agard, P., De Hoog, J. C. M., Omrani, J., and Plunder, A., 2013, Insights on deep, accretionary subduction processes from the Sistan ophiolitic "melange" (Eastern Iran): Lithos, v. 156–159, p. 139–158, https://doi.org/10.1016/j.lithos.2012.11.007

Barrat, J. A., Joron, J. L., Taylor, R. N., Fourcade, S., Nesbitt, R. W., and Jahn, B. M., 2003, Geochemistry of basalts from Manda Hararo, Ethiopia: LREE-depleted basalts in Central Afar: Lithos, v. 69, n. 1–2, p. 1–13, https://doi.org/10.1016/S0024-4937(03)00044-6

Barth, M. G., McDonough, W. F., and Rudnick, R. L., 2000, Tracking the budget of Nb and Ta in the continental crust: Chemical Geology, v. 165, n. 3–4, p. 197–213, https://doi.org/10.1016/S0009-2541(99)00173-4

Bédard, J. H., and Stevenson, R. 1999. The Caldwell Group lavas of southern Quebec: MORB-like tholeiites associated with the opening of Iapetus Ocean: Canadian Journal of Earth Sciences, v. 36, n. 6, p. 999–1019, https://doi.org/10.1139/e99-018

Bédard, J. H., and Wilson, C., 1997, Fractionation and contamination of Maquereau Group lavas, southern Gaspé, Québec Appalachians, *in* Sinha, A. K., Whalen, J. B., and Hogan, J. P., editors, The Nature of Magmatism in the Appalachian Orogen: Geological Society of America Memoir 191, p. 87–106, https://doi.org/10.1130/0-8137-1191-6.87

Bédard, J. H., Lauzière, K., Tremblay, A., and Sangster, A., 1998, Evidence for forearc seafloor-spreading from the Betts Cove ophiolite, Newfoundland: Oceanic crust of boninitic affinity: Tectonophysics, v. 284, n. 3–4, p. 233–245, https://doi.org/10.1016/S0040-1951(97)00182-0

Bothner, W. A., and Laird, J., 1999, Geologic map of the Tillotson Peak-Haystack area, Hazens Notch and parts of the Lowell 7.5 minute quadrangles, Vermont: Vermont Geological Survey Open File Report VG99-5.

Burton, W. C., and Southworth, S., 2010, A model for Iapetan rifting of Laurentia based on Neoproterozoic dikes and related rocks, *in* Tollo, R., Bartholomew, M. J., Hibbard, J. P., and Karabinos, P. M., editors, From Rodinia to Pangea: The Lithotectonic Record of the Appalachian Region: Geological Society of America Memoir 206, p. 455–476, https://doi.org/10.1130/2010.1206(20)

Cabanis, B., and Lecolle, M., 1989, Le diagramme La/10-Y/15-Nb/8: un outil pour la discrimination des séries volcaniques et la mise en évidence des processus de mélange et/ou de contamination crustale: Comptes rendus de l'Académie des sciences, Série 2, Mécanique, Physique, Chimie, Sciences de l'univers, Sciences de la Terre, v. 309, p. 2023–2029.

Castonguay, S., Kim, J., Thompson, P. J., Gale, M. H., Joyce, N., Laird, J., and Doolan, B. L., 2012, Timing of tectonometamorphism across the Green Mountain anticlinorium, northern Vermont Appalachians: $^{40}Ar/^{39}Ar$ data and correlations with southern Quebec: Geological Society of America Bulletin, v. 124, n. 3–4, p. 352–367, https://doi.org/10.1130/B30487.1

Castonguay, S., van Staal, C. R., Joyce, N., Skulski, T., and Hibbard, J. P., 2014, Taconic Metamorphism Preserved in the Baie Verte Peninsula, Newfoundland Appalachians: Geochronological Evidence for Ophiolite Obduction and Subduction and Exhumation of the Leading Edge of the Laurentian (Humber) Margin During Closure of the Taconic Seaway: Geoscience Canada, v. 41, n. 4, http://dx.doi.org/10.12789/geocanj.2014.41.055

Cawood, P. A., Dunning, G. R., Lux, D., and van Gool, J. A. M., 1994, Timing of peak metamorphism and deformation along the Appalachian margin of Laurentia in Newfoundland: Silurian, not Ordovician: Geology, v. 22, n. 5, p. 399–402, https://doi.org/10.1130/0091-7613(1994)022<0399:TOPMAD>2.3.CO;2

Cawood, P. A., McCausland, P. J. A., and Dunning, G. R., 2001, Opening Iapetus: Constraints from the Laurentian margin in Newfoundland: Geological Society of America Bulletin, v. 113, n. 4, p. 443–453, https://doi.org/10.1130/0016-7606(2001)113<0443:OICFTL>2.0.CO;2

Coish, R. A., 1997, Rift and ocean floor volcanism from the Late Proterozoic and early Paleozoic of the Vermont Appalachians, *in* Sinha, A. K., Whalen, J. B., and Hogan, J. P., editors, The Nature of Magmatism in the Appalachian Orogen: Geological Society of America Memoir 191, p. 129–145, https://doi.org/10.1130/0-8137-1191-6.129

——— 2010, Magmatism in the Vermont Appalachians, *in* Tollo, R., Bartholomew, M. J., Hibbard, J. P., and Karabinos, P. M., editors, From Rodinia to Pangea: The Lithotectonic Record of the Appalachian Region: Geological Society of America Memoir 206, p. 91–110, https://doi.org/10.1130/2010.1206(05)

Coish, R. A., and Gardner, P., 2004, Suprasubduction-zone peridotite in the Northern USA Appalachians: Evidence from mineral composition: Mineralogical Magazine, v. 68, n. 4, p. 699–708, https://doi.org/10.1180/0026461046840214

Coish, R. A., and Sinton, C. W., 1992, Geochemistry of mafic dikes in the Adirondack Mountains: Implications for Late Proterozoic continental rifting: Contributions to Mineralogy and Petrology, v. 110, n. 4, p. 500–514, https://doi.org/10.1007/BF00344084

Coish, R. A., Hickey, R., and Frey, F. A., 1982, Rare earth element geochemistry of the Betts Cove ophiolite,

Newfoundland: Complexities in ophiolite formation: Geochimica et Cosmochimica Acta, v. 46, n. 11, p. 2117–2134, https://doi.org/10.1016/0016-7037(82)90189-2
Coish, R. A., Fleming, F. S., Larsen, M., Poyner, R., and Seibert, J., 1985, Early rift history of the proto-Atlantic ocean: Geochemical evidence from metavolcanic rocks in Vermont: American Journal of Science, v. 285, n. 4, p. 351–378, https://doi.org/10.2475/ajs.285.4.351
Coish, R. A., Perry, D. A., Anderson, C. D., and Bailey, D., 1986, Metavolcanic rocks from the Stowe Formation, Vermont: Remnants of ridge and intraplate volcanism in the Iapetus ocean: American Journal of Science, v. 286, n. 1, p. 1–28, https://doi.org/10.2475/ajs.286.1.1
Coish, R. A., Bramley, A., Gavigan, T., and Masinter, R. A., 1991, Progressive changes in volcanism during Iapetan rifting: Comparisons with the East African Rift-Red Sea system: Geology, v. 19, n. 10, p. 1021–1024, https://doi.org/10.1130/0091-7613(1991)019<1021:PCIVDL>2.3.CO;2
Coish, R. A., Kim, J., Morris, N., and Johnson, D., 2012, Late stage rifting of the Laurentian continent: Evidence from the geochemistry of greenstone and amphibolite in the central Vermont Appalachians: Canadian Journal of Earth Sciences, v. 49, n. 1, p. 43–58, https://doi.org/10.1139/e11-013
Coish, R., Kim, J., Twelker, E., Zolkos, S., and Walsh, G., 2015, Geochemistry and origin of metamorphosed mafic rocks from the lower Paleozoic Moretown and Cram Hill formations of north-central Vermont: Delamination magmatism in the western New England Appalachians: American Journal of Science, v. 315, n. 9, p. 809–845, https://doi.org/10.2475/09.2015.02
David, J., and Marquis, R., 1994, Géochronologie U-Pb dans les Appalaches du Québec: Application aux roches de la zone de Dunnage: La Revue Géologique, v. 1, p. 16–20.
DePaolo, D. J., 1981, Neodymium isotopes in the Colorado Front Range and crust-mantle evolution in the Proterozoic: Nature, v. 291, p. 193–196, https://doi.org/10.1038/291193a0
DePaolo, D. J., and Wasserburg, G. J., 1976, Nd isotopic variations and petrogenetic models: Geophysical Research Letters, v. 3, n. 5, p. 249–252, https://doi.org/10.1029/GL003i005p00249
De Souza, S., Tremblay, A., Daoust, C., and Gauthier, M., 2008, Stratigraphy and geochemistry of the Lac-Brompton ophiolite, Canada: Evidence for extensive forearc magmatism and mantle exhumation in the Southern Quebec Ophiolite Belt: Canadian Journal of Earth Sciences, v. 45, n. 9, p. 999–1014, https://doi.org/10.1139/E08-044
Doolan, B. L., Gale, M. H., Gale, P. N., and Hoar, R. S., 1982, Geology of the Quebec Reentrant: Possible constraints from early rifts and the Vermont–Quebec serpentine belt, *in* St. Julien, P., and Beland, J., editors, Major Structural Zones and Faults of the Northern Appalachians: Geological Association of Canada Special Paper 7, p. 87–115.
Dorais, M. J., Marvinney, R. G., and Markert, K., 2017, The age, petrogenesis and tectonic significance of the Frontenac Formation basalts, northern New Hampshire and western Maine: American Journal of Science, v. 317, n. 9, p. 990–1018, https://doi.org/10.2475/09.2017.02
Dostal, J., Wilson, R. A., and Keppie, J. D., 1989, Geochemistry of Siluro-Devonian Tobique volcanic belt in northern and central New Brunswick (Canada): Tectonic implications: Canadian Journal of Earth Sciences, v. 26, n. 6, p. 1282–1296, https://doi.org/10.1139/e89-108
Dunning, G. R., and Krogh, T. E., 1985, Geochronology of ophiolites of the Newfoundland Appalachians: Canadian Journal of Earth Sciences, v. 22, n. 11, p. 1659–1670, https://doi.org/10.1139/e85-174
Dunning, G. R., and Pedersen, R. B., 1988, U/Pb ages of ophiolites and arc-related plutons of the Norwegian Caledonides: Implications for the development of Iapetus: Contributions to Mineralogy and Petrology, v. 98, n. 1, p. 13–23, https://doi.org/10.1007/BF00371904
Fitton, J. G., 2007, The OIB paradox, *in* Foulger, G. R., and Jurdy, D. M., editors, Plates, plumes, and planetary processes: Geological Society of America Special Paper 430, p. 387–412, https://doi.org/10.1130/2007.2430(20)
Fitton, J. G., Saunders, A. D., Norry, M. J., Hardarson, B. S., and Taylor, R. N., 1997, Thermal and chemical structure of the Iceland plume: Earth and Planetary Science Letters, v. 153, n. 3–4, p. 197–208, https://doi.org/10.1016/S0012-821X(97)00170-2
Floyd, P. A., and Winchester, J. A., 1978, Identification and discrimination and altered and metamorphosed volcanic rocks using immobile elements: Chemical Geology, v. 21, n. 3–4, p. 291–306, https://doi.org/10.1016/0009-2541(78)90050-5
Gale, M. H., 1980, Geology of the Belvidere Mountain Complex, Eden and Lowell, Vermont: U.S. Geological Survey Open-File Report 80-978, 169 p., https://doi.org/10.3133/ofr80978
——— 1986, Geologic map of the Belvidere Mountain area, Eden and Lowell, Vermont: United States Geological Survey, scale 1:24,000.
——— 2007, Bedrock geologic map of the Hazens Notch and portions of the Eden and Lowell 7.5 minute quadrangles, Vermont: Vermont Geological Survey, scale 1:24,000.
Guillot, S., Schwartz, S., Reynard, B., Agard, P., and Prigent, C., 2015, Tectonic significance of serpentinites: Tectonophysics, v. 646, p. 1–19, https://doi.org/10.1016/j.tecto.2015.01.020
Hashiguchi, H., Yamada, R., and Inoue, 1983, Practical application of low Na_2O anomalies in footwall acid lava for delimiting promising areas around the Kosaka and Fukazawa Kuroko deposits, Akita Prefectural, Japan, *in* Ohmoto, H., and Skinner, B. J., editors, The Kuroko massive sulfide deposits: Economic Geology, Monograph 5, p. 387–394.
Hatch, N. L., Jr., and Stanley, R. S., 1976, Geologic map of the Blandford quadrangle, Hampden and Hampshire Counties, Massachusetts: U.S. Geological Survey Geologic Quadrangle Map GQ-1312, scale 1:24,000.
Hibbard, J. P., 1983, Geology of the Baie Verte Peninsula, Newfoundland: Mineral Development division Department of Mines and Energy, Government of Newfoundland and Labrador, Memoir 2, 279 p.
Hibbard, J. P., van Staal, C. R., Rankin, D. W., and Williams, H., 2006, Lithotectonic map of the Appalachian Orogen: Geological Survey of Canada Map 2096A, scale 1:1,500,000.
Hibbard, J. P., van Staal, C. R., and Rankin, D. W., 2007, A comparative analysis of pre-Silurian crustal

building blocks of the northern and the southern Appalachian orogen: American Journal of Science, v. 307, n. 1, p. 23-45, https://doi.org/10.2475/01.2007.02
Honsberger, I. W., ms, 2015, Metamorphism, deformation, geochemistry, and tectonics of exhumed ultramafic and mafic rocks in the central and north-central Vermont Appalachians: Durham, New Hampshire, University of New Hampshire, Durham, Ph. D. thesis, 193 p.
Honsberger, I. W., Laird, J., and Thompson, P. J., 2017, A tectonized ultramafic-mafic-pelitic package in Stockbridge, Vermont: Metamorphism resulting from subduction and exhumation: American Journal of Science, v. 317, n. 9, p. 1019–1047, https://doi.org/10.2475/09.2017.03
Humphris, S. E., and Thompson, G., 1978, Hydrothermal alteration of oceanic basalts by seawater: Geochimica et Cosmochimica Acta, v. 42, n. 1, p. 107–125, https://doi.org/10.1016/0016-7037(78)90221-1
Jacobi, R. D., and Mitchell, C., 2018, Aseismic-ridge subduction as a driver for the Ordovician Taconic orogeny and Utica foreland basin in New England and New York State, *in* Ingersoll, R. V., Lawton, T. F., and Graham, S. A., editors, Tectonics, Sedimentary Basins and Provenance: A Celebration of William R. Dickinson's Career: Geological Society of America Special Paper 540, p. 617–659, https://doi.org/10.1130/2018.2540(27)
Jenner, G. A., Dunning, G. R., Malpas, J., Brown, M., and Brace, T., 1991, Bay of Islands and Little Port complexes, revisited: Age, geochemical and isotopic evidence confirm suprasubduction-zone origin: Canadian Journal of Earth Sciences, v. 28, n. 10, p. 1635–1652, https://doi.org/10.1139/e91-146
Karabinos, P., Macdonald, F. A., and Crowley, J. L., 2017, Bridging the gap between the foreland and hinterland I: Geochronology and plate tectonic geometry of Ordovician magmatism and terrane accretion on the Laurentian margin of New England: American Journal of Science, v. 317, n. 5, p. 515–554, https://doi.org/10.2475/05.2017.01
Kim, J., and Jacobi, R. D., 1996, Geochemistry and tectonic implications of Hawley Formation meta-igneous units: Northwestern Massachusetts: American Journal of Science, v. 296, n. 10, p. 1126–1174, https://doi.org/10.2475/ajs.296.10.1126
——— 2002, Boninites: Characteristics and tectonic constraints, northeastern Appalachians: Physics and Chemistry of the Earth, Parts A/B/C, v. 27, n. 1–3, p. 109–147, https://doi.org/10.1016/S1474-7065(01)00005-5
Kim, J., Coish, R., Evans, M., and Dick, G., 2003, Supra-subduction zone extensional magmatism in Vermont and adjacent Quebec: Implications for early Paleozoic Appalachian tectonics. Geological Society of America Bulletin, v. 115, n. 12, p. 1552–1569, https://doi.org/10.1130/B25343.1
Kumarapeli, P. S., Dunning, G. R., Pintson, H., and Shaver, J., 1989, Geochemistry and U-Pb zircon age of comenditic metafelsites of the Tibbit Hill Formation, Quebec Appalachians: Canadian Journal of Earth Sciences, v. 26, n. 7, p. 1374–1383, https://doi.org/10.1139/e89-117
Lafléche, M. R., Schrijver, K., and Tremblay, A., 1993, Geochemistry, origin, and provenance of Upper Proterozoic to Upper Cambrian alkaline to transitional basaltic rocks in and contiguous to a sector of the Appalachian Humber zone, Canada: American Journal of Science, v. 293, n. 9, p. 980–1009, https://doi.org/10.2475/ajs.293.9.980
Laird, J., and Albee A. L., 1981a, High pressure metamorphism in mafic schist from northern Vermont: American Journal Science, v. 281, n. 2, p. 97–126, https://doi.org/10.2475/ajs.281.2.97
——— 1981b, Pressure, temperature, and time indicators in mafic schist: Their application to reconstructing the polymetamorphic history of Vermont: American Journal Science, v. 281, n. 2, p. 127–175, https://doi.org/10.2475/ajs.281.2.127
Laird, J., and Honsberger, I. W., 2013, Taconian subduction: Pressure, temperature paths preserved in metamorphosed mafic rocks from northern Vermont and adjacent Quebec: Geological Society of America Abstracts with Programs, v. 45, n. 1, p. 106.
Laird, J., Lanphere, M. A., and Albee, A. L., 1984, Distribution of Ordovician and Devonian metamorphism in mafic and pelitic schists from northern Vermont: American Journal of Science, v. 284, n. 4–5, p. 376–413, https://doi.org/10.2475/ajs.284.4-5.376
Laird, J., Trzcienski, W. E., Jr., and Bothner, W. A., 1993, High-pressure, Taconian, and subsequent polymetamorphism of southern Quebec and northern Vermont, *in* Cheney, J. T., and Hepburn, J. C., editors, Field trip Guidebook for the Northeastern United States: Geological Society of America field trip, v. 2, p. 1–32.
Laird, J., Bothner, W. A., Thompson, P. J., Thompson, T., Gale, M., and Kim, J., 2001, Geochemistry, petrology, and structure of the Tillotson Peak and Belvidere Mountain mafic complexes, northern Vermont: Geological Society of America Abstracts with Programs, v. 33, n. 1, p. A59.
Lugmair, G. W., 1974, Sm Nd ages: A new dating method (abstract): Meteoritics, v. 9, p. 369.
Macdonald, F. A., Ryan-Davis, J., Coish, R. A., Crowley, J. L., and Karabinos, P., 2014, A newly identified Gondwanan terrane in the northern Appalachian Mountains: Implications for the Taconic orogeny and closure of the Iapetus Ocean: Geology, v. 42, n. 6, p. 539–542, https://doi.org/10.1130/G35659.1
Macdonald, F. A., Karabinos, P. M., Crowley J. L., Hodgin, E. B., Crockford, P. W., and Delano J. W., 2017, Bridging the gap between the foreland and hinterland II: Geochronology and tectonic setting of Ordovician magmatism and basin formation on the Laurentian margin of New England and Newfoundland: American Journal of Science, v. 317, n. 5, p. 555–596, https://doi.org/10.2475/05.2017.02
McDonough, W. F., and Sun, S.-S., 1995, The composition of the Earth: Chemical Geology, v. 120, n. 3–4, p. 223–253, https://doi.org/10.1016/0009-2541(94)00140-4
Mélancon, B., Hébert, R., Laurent, R., and Dostal, J., 1997, Petrological and geochemical characteristics of the Bolton Igneous Group, southern Quebec Appalachians: American Journal of Science, v. 297, n. 5, p. 527–549, https://doi.org/10.2475/ajs.297.5.527
Mottl, M. J., 1983, Metabasalts, axial hot springs, and the structure of hydrothermal systems at mid-ocean

ridges: Geological Society of America Bulletin, v. 94, n. 2, p. 161–180, https://doi.org/10.1130/0016-7606(1983)94<161:MAHSAT>2.0.CO;2
Murphy, J. B., Cousens, B. L., Braid, J. A., Strachan, R. A., Dostal, J., Keppie, J. D., and Nance, R. D., 2011, Highly depleted oceanic lithosphere in the Rheic Ocean: Implications or Paleozoic plate reconstructions: Lithos, v. 123, n. 1–4, p. 165–175, https://doi.org/10.1016/j.lithos.2010.09.014
Murphy, J. B., Waldron, J. W. F., Schofield, D. I., Barry, T. L., and Band, A. R., 2014, Highly depleted isotopic compositions evident in Iapetus and Rheic Ocean basalts: Implications for crustal generation and preservation: International Journal of Earth Sciences, v. 103, n. 5, p. 1219–1232, https://doi.org/10.1007/s00531-013-0925-1
Murton, B. J., Sauter, D., Milton, J. A., and Tindle, A. G., 2005, Heterogeneity in southern Central Indian Ridge MORB: Implications for ridge-hot spot interaction: Geochemistry, Geophysics, Geosystems, v. 6, Q03E20, http://dx.doi.org/10.1029/2004GC000798
Pearce, J. A., 2008, Geochemical fingerprinting of oceanic basalts with applications to ophiolite classification and the search for Archean oceanic crust: Lithos, v. 100, n. 1–4, p. 14–48, https://doi.org/10.1016/j.lithos.2007.06.016
Pearce, J. A., and Norry, M. J., 1979, Petrogenetic implications of Ti, Zr, Y and Nb variations in volcanic rocks: Contributions to Mineralogy and Petrology, v. 69, n. 1, p. 33–47. https://doi.org/10.1007/BF00375192
Puffer, J. H., 2002, A Late Neoproterozoic eastern Laurentian superplume: Location, size, chemical composition, and environmental impact: American Journal of Science, v. 302, n. 1, p. 1–27, https://doi.org/10.2475/ajs.302.1.1
Rankin, D. W., 1976, Appalachian salients and recesses: Late Precambrian continental breakup and opening of the Iapetus Ocean: Journal of Geophysical Research, v. 81, n. 32, p. 5605–5619, https://doi.org/10.1029/JB081i032p05605
Rankin, D. W., Coish, R. A., Tucker, R. D., Peng, Z. X., Wilson, S. A., and Rouff, A. A., 2007, Silurian extension in the Upper Connecticut Valley, United States and the origin of middle Paleozoic basins in the Québec Embayment: American Journal of Science, v. 307, n. 1, p. 216–264, https://doi.org/10.2475/01.2007.07
Ratcliffe, N. M., Stanley, R. S, Gale, M. H., Thompson, P. J., and Walsh, G. J., 2011, Bedrock Geologic Map of Vermont: U.S. Geological Survey Scientific Investigations Map 3184, 3 sheets, scale 1:100,000.
Richard, P., Shimizu, N., and Allégre, C. J., 1976, $^{143}Nd/^{144}Nd$, a natural tracer: An application to oceanic basalts: Earth and Planetary Science Letters, v. 31, n. 2, p. 269–278, https://doi.org/10.1016/0012-821X(76)90219-3
Rodgers, J., 1970, The Tectonics of the Appalachians: New York, Wiley-Interscience, 271 p.
Rollinson, H., 1993, Using geochemical data: Evaluation, presentation, interpretation: New York, New York, John Wiley & Sons, 352 p.
Rudnick, R. L., and Fountain, D. M., 1995, Nature and composition of the continental crust–A lower crustal perspective: Reviews of Geophysics, v. 33, n. 3, p. 267–309, https://doi.org/10.1029/95RG01302
Schroetter, J.-M., Bédard, J. H., and Tremblay, A., 2005, Structural evolution of the Thetford Mines Ophiolitic Complex, Canada: Implications for the southern Québec ophiolitic belt: Tectonics, v. 24, n. 1, p. 1–20, https://doi.org/10.1029/2003TC001601
Shaw, H. F., and Wasserburg, G. J., 1984, Isotopic constraints on the origin of Appalachian mafic complexes: American Journal of Science, v. 284, n. 5, p. 319–349, https://doi.org/10.2475/ajs.284.4-5.319
Stanley, R. S., and Hatch, N. L., Jr., 1988, The pre-Silurian geology of the Rowe-Hawley Zone, *in* Hatch, N. L., Jr., editor, The Bedrock Geology of Massachusetts: U. S. Geological Survey Professional Paper P 1366 A-D, p. A1–A3.
Stanley, R. S., and Ratcliffe, N. M., 1985, Tectonic synthesis of the Taconian orogeny in western New England: Geological Society of America Bulletin, v. 96, n. 10, p. 1227–1250, https://doi.org/10.1130/0016-7606(1985)96<1227:TSOTTO>2.0.CO;2
Stanley, R. S., Roy, D. L., Hatch, N. L., and Knapp, D. A., 1984, Evidence for tectonic emplacement of ultramafic and associated rocks in the pre-Silurian eugeoclinal belt of western New England; vestiges of an ancient accretionary wedge: American Journal of Science, v. 284, n. 4–5, p. 559–595, https://doi.org/10.2475/ajs.284.4-5.559
Sun, S. -S., and McDonough, W. F., 1989, Chemical and isotopic systematics of oceanic basalts: Implications for mantle composition and processes: Geological Society, London, Special Publications, v. 42, p. 313–345, https://doi.org/10.1144/GSL.SP.1989.042.01.19
Thomas, W. A., 2014, A mechanism for tectonic inheritance at transform faults of the Iapetan margin of Laurentia: Geoscience Canada, v. 41, n. 3, p. 321–344, https://doi.org/10.12789/geocanj.2014.41.048
Thompson, A. B., and Laird, J., 2005, Calibrations of modal space for metamorphism of mafic schist: American Mineralogist, v. 90, n. 5–6, p. 843–856, https://doi.org/10.2138/am.2005.1717
Thompson, P. J., and Thompson, T. B., 2003, The Prospect Rock thrust: Western limit of the Taconian accretionary prism in the northern Green Mountain Anticlinorium, Vermont: Canadian Journal of Earth Sciences, v. 40, n. 2, p. 269–284, https://doi.org/10.1139/e02-109
Thompson, J. B., Jr., Laird J., and Thompson, A. B., 1982, Reactions in amphibolite, greenschist and blueschist: Journal of Petrology, v. 23, n. 1, p. 1–27, https://doi.org/10.1093/petrology/23.1.1
Tremblay, A., and Pinet, N., 1994, Distribution and characteristics of the Taconian and Acadian deformation, southern Québec Appalachians: Geological Society of America Bulletin, v. 106, n. 9, p. 1172–1181, https://doi.org/10.1130/0016-7606(1994)106<1172:DACOTA>2.3.CO;2
——— 2016, Late Neoproterozoic to Permian tectonic evolution of the Quebec Appalachians, Canada: Earth-Science Reviews, v. 160, p. 131–170, https://doi.org/10.1016/j.earscirev.2016.06.015
van Staal, C. R., and Barr, S. M., 2012, Lithospheric architecture and tectonic evolution of the Canadian Appalachians and associated Atlantic margin, *in* Percival, J. A., Cook, F. A., and Clowes, R. M., editors,

Tectonic Styles in Canada Revisited: The LITHOPROBE Perspective: Geological Association of Canada Special Paper 49, p. 41–95.
van Staal, C. R., Dewey, J. F., Mac Niocaill, C., and McKerrow, W. S., 1998, The Cambrian-Silurian tectonic evolution of the northern Appalachians and British Caledonides: History of a complex, west and southwest Pacific-type segment of Iapetus, *in* Blundell, D. J., and Scott, A. C., editors, Lyell: The Past Is the Key to the Present: Geological Society of London Special Publication 143, p. 199–242, https://doi.org/10.1144/GSL.SP.1998.143.01.17
van Staal, C. R., Currie, K. L., Rowbotham, G., Goodfellow, W., and Rogers, N., 2008, Pressure-temperature paths and exhumation of Late Ordovician–Early Silurian blueschists and associated metamorphic nappes of the Salinic Brunswick subduction complex, northern Appalachians: Geological Society of America Bulletin, v. 120, n. 11–12, p. 1455–1477, https://doi.org/10.1130/B26324.1
Walsh, G. J., and Aleinikoff, J. N., 1999, U–Pb zircon age of metafelsite from the Pinney Hollow Formation: Implications for the development of the Vermont Appalachians: American Journal of Science, v. 299, n. 2, p. 157–170, https://doi.org/10.2475/ajs.299.2.157
Walsh, G. J., and Falta, C. K., 2001, Bedrock geologic map of the Rochester quadrangle, Rutland, Windsor, and Addison Counties, Vermont: U.S. Geological Survey Scientific Investigations Map I-2626, scale 1:24,000.
Walsh, G. J., Kim, J., Gale, M. H., and King, S. M., 2010, Bedrock geologic map of the Montpelier and Barre West quadrangles, Washington and Orange Counties, Vermont: U.S. Geological Survey Scientific Investigations Map 3111,scale 1:24,000.
Westerman, D. S., 1987, Structures in the Dog River fault zone between Northfield and Montpelier, Vermont, *in* Westerman, D. S., editor, New England Intercollegiate Geological Conference: Guidebook for Field Trips in Vermont, 79th Annual Meeting, v. 2, p. 109–132.
Williams, H., 1979, Appalachian orogen in Canada: Canadian Journal of Earth Sciences, v. 16, n. 3, p. 792–807, https://doi.org/10.1139/e79-070
——— 1995, Temporal and spatial subdivisions of the rocks of the Canadian Appalachian region, *in* Williams, H., editor, Geology of the Appalachian-Caledonian Orogen in Canada and Greenland: Geological Survey of Canada, Geology of Canada, n. 6, p. 21–44, https://doi.org/10.4095/205242
Williams, H., and St. Julien, P., 1982, The Baie Verte-Brompton Line: Early Paleozoic continent ocean interface in the Canadian Appalachians, *in* St. Julien, P., and Béland, J., editors, Major Structural Zones and Faults of the Northern Appalachians: Geological Association of Canada Special Paper 24, p. 178–206.
Williams, H., Colman-Sadd, S. P., and Swinden, H. S., 1988, Tectono-stratigraphic subdivisions of central Newfoundland: Current Research, Part B, Geological Survey of Canada Paper 88-1B, p. 91–98.
Wilson, M., 1989, Igneous Petrogenesis: London, Unwin-Hyman, 466 p.
Zagorevski, A., van Staal, C. R., McNicoll, V., Rogers, N., and Valverde-Vaquero, P., 2007, Tectonic architecture of an arc-arc collision zone, Newfoundland Appalachians, *in* Draut, A. E., Clift, P. D., and Scholl, D. W., editors, Formation and Applications of the Sedimentary Record in Arc Collision Zones: Geological Society of America Special Paper 436, p. 309–333, https://doi.org/10.1130/2008.2436(14)